Table 1
The accession numbers of TLRs and innate immunity genes used for BLAST and phylogenetic analyses. The accession numbers of NCBI are listed. Only *X. tropicalis* TLRs are indicated by JGI ID.

Species	Gene name			
Homo sapiens	TLR1 (U88540)	TLR2 (U88878)	TLR3 (U88879)	TLR4 (U88880)
	TLR5 (NM_003268)	TLR6 (NM_006068)	TLR7 (NM_016562)	TLR8 (NM_016610)
	TLR9 (AF259262)	TLR10 (AF296673)	MyD88 (NP_002459.1)	TICAM-1 (AB086380)
	TICAM-2 (NP_067681.1)	TIRAP (NP_001034750.1)	SARM (NP_055892.2)	LBP (NP_004130.2)
	CD14 (NP_001035110.1)	MD2 (NP_056179.2)	RIG-I (AF038963)	MDA5 (AF095844)
	LGP2 (NP_077024.2)	IPS-1 (NP_065797.2)	IRAK1 (NM_001025242)	IRAK2 (NM_001025242)
	IRAK3 (NP_001135995.1)	IRAK4 (NM_001114182)	TRAF3 (NM_003300)	TRAF6 (NM_004620)
	TAB2 (NM_015093)	TAB3 (NM_152787)	TBK1 (NP_037386.1)	RIP1 (NP_003795)
	CASP8 (NP_001219.2)	FADD (NP_003815.1)	TANK (NP_004171.2)	SINTBAD (NP_055541.1)
	IKKα (NP_001269.3)	IKKβ (NP_001547.1)	IKKγ (NP_001093327.1)	IKKε (NP_054721.1)
	NAP1 (NP_071906.1)	MKK6 (NP_002749.2)	MKK3 (NP_002747.2)	JNK (NP_002741)
	TAB2 (NM_015093)	IRF3 (NP_001562.1)	IRF7 (NP_001563.2)	RELA (NP_001138610.1)
	NFκB1 (NP_001158884.1)	ATF2 (NP_001871.2)	AP-1 (NP_034721.1)	Mx (NM_001144925)
	PKR (NM_001135651)	OAS1 (NM_001032409)	IFNα (NM_024013)	IFNβ (NM_002176)
	TNFα (NP_000585)	IL-6 (NM_000600)	IL-12p40 (NP_002178.2)	
M. musculus	TLR1 (NM_030682)	TLR2 (NM_011905.3)	TLR3 (NM_126166)	TLR4 (NM_021297)
	TLR5 (NM_016928)	TLR6 (NM_011604)	TLR7 (NM_133211)	TLR8 (NM_133212)
	TLR9 (NM_031178)	TLR11 (NM_205819)	TLR12 (NM_205823)	TLR13 (NM_205820)
	MyD88 (NP_034981.1)	TICAM-1 (NP_778154.1)	TICAM-2 (NP_775570.1)	TIRAP (NP_473437.1)
	SARM (NP_766383.2)			
G. gallus	TLR1 (NM_001007488)	TLR2 (NM_204278)	TLR3 (NM_001011691)	TLR4 (NM_001030693)
	TLR5 (NM_001024586)	TLR6 (NM_001007488)	TLR7 (NM_001011688)	TLR15 (NM_001037835)
	TLR21 (NM_001030558)	MyD88 (NP_001026133.1)	TICAM-1 (NM_001081506)	TIRAP (NP_001020000.1)
	SARM (XP_415814.2)			
X. tropicalis	TLR1 (jgi371271)	TLR2.1 (jgi320872)	TLR2.2 (jgi320954)	TLR3 (jgi271893)
	TLR5 (jgi459490)	TLR6.1 (jgi281677)	TLR6.2 (jgi371307)	TLR7 (jgi323633)
	TLR8.1 (jgi161716)	TLR8.2 (jgi323721)	TLR9 (jgi350411)	TLR12 (jgi187046)
	TLR14.1 (jgi190020)	TLR14.2 (jgi30694)	TLR14.3 (jgi421728)	TLR14.4 (jgi421736)
	TLR21 (jgi349648)	TLR22 (jgi414791)	MyD88 (DR867184)	TICAM-1 (CX999107.1)
	TIRAP (NM_001044460)			
D. rerio	TLR1 (XM_692439)	TLR2 (NM_212812.1)	TLR3 (AY616582)	TLR4a (NM_001131051)
	TLR4b (NM_212813)	TLR5a (XP_001919052)	TLR5b (XM_001343113)	TLR7 (XP_701101.3)
	TLR8a (XP_001920594)	TLR8b (XM_001340150)	TLR9 (XM_685911)	TLR12 (XM_685162)
	TLR14 (NM_001089350)	TLR18(BC162732)	TLR21 (XP_001923227.1)	TLR22 (XM_692565)
	MyD88 (NP_997979.2)	TICAM-1 (NP_001038224.1)	TIRAP (XP_001922965.1)	SARM (XP_001344407.1)
T. rubripes	TLR1 (AAW69368)	TLR2 (AAW69370)	TLR3 (AC156436)	TLR5 (AC156437)
	TLR5S (AC156440)	TLR7 (AC156438)	TLR8 (AC156438)	TLR9 (AC156439)
	TLR14 (AC156431)	TLR21 (NM_001032579)	TLR22 (NM_001113193)	TLR23 (AC156435)
	MyD88 (NM_001113195)	TICAM-1(NM_001113194)	TIRAP (NM_001113196)	
Lethentron japonicum	TLR14a (AB109402)	TLR14b (AB109403)		

(pmTLRs) (Fig. 1). The other 4 proteins were defined as TLR adaptor-like proteins since they are similar to MyD88, TICAM or SARM.

Based on the Genscan ID and EST accession numbers, the contig positions and *E*-values for the 16 pmTLR proteins were determined, and each protein was annotated based on their most likely TLR homolog (Table 2). Sea lamprey pmTLR14a and pmTLR14b were most homologous to Japanese lamprey laTLR14a (ljTLR14a) and laTLR14b (ljTLR14b), respectively, which we previously identified (Ishii et al., 2007b). An additional two genes, pmTLR14c and pmTLR14d, encoded paralogs of ljTLR14a and b, and were more homologous to zebrafish TLR18 than any other TLR family member. Additionally, we found four TLR2-like genes formed a unique cluster independent of the clade of the mammalian TLR2 (Fig. 2). Therefore, we designated these pmTLR genes TLR24a-d, which represent a novel TLR2 subfamily. TLR2c and d both localized to contig 1344, suggesting a cause of gene duplication, however, the presence of an ambiguous gap between the two genes deterred us from concluding that they originated from a tandem duplication. It is notable that the TLR7/8, TLR14, and TLR21 genes were mapped to distinct contigs. Although pmTLR2c appeared to be an ortholog of *Canis lupus* TLR6, its functional similarity to mammalian TLR6 could not be determined. Lamprey possessed orthologous genes for TLR3, TLR5, TLR7, and TLR8 but not for TLR4 or TLR9. In addition to the M-type TLRs, three TLR21 and a single TLR22 orthologs classified as F-type TLRs were identified in the lamprey genome database. Taken together, the phylogenetic analyses revealed that sea lamprey has a TLR system comprised of an incomplete set of M-type and full F-type TLRs, as in fish (Fig. 1).

Although many animal TLR genes are predicted to be intronless (Roach et al., 2005), *T. rubripes* TLR genes have been reported to contain introns and be dispersed over wide regions on a variety of chromosomes (Oshiumi et al., 2003a). In the Pre-Ensemble Lamprey Genome database, lamprey TLR2d, 3, 14c, 22, and 24d contain several introns in coding regions, while TLR2a, 2b, 14a, 14b, 21a, 21b, 21c, 24a and 24b are intronless. As only partial sequences for TLR2c, 5, 7, 8a, 8b, 14d, and 24c were obtained from the genome database, it was impossible to conclusively determine if introns were present. Nevertheless, the results infer that lamprey TLRs are encoded by both intron-containing and intronless genes, as is the case in teleosts (Oshiumi et al., 2003a).

Using the SMART program, typical TLR structures of pmTLR proteins were predicted (Fig. 1). Almost all proteins consisted of multiple LRRs in the N-terminal region and a single TIR domain in the C-terminus, split by a transmembrane domain. Although we failed to detect the N- or C-terminal regions in several pmTLRs, their mRNAs, except for TLR24c, were detected by RT-PCR, suggesting that the mRNAs of these pmTLRs are present as complete forms but their signal peptides and N-terminal LRRs could not be

Please cite this article in press as: Kasamatsu, J., et al., Phylogenetic and expression analysis of lamprey toll-like receptors. Dev Comp Immunol (2010), doi:10.1016/j.dci.2010.03.004

Table 2
Annotation of TLR and other innate immunity genes in the *P. marinus* genome. Each TLR and other innate immune gene was annotated using a BLASTP search and described as a TLR after meeting specific criteria. The encoded contig numbers and *E*-value are shown.

Gene categories	Gene name (*P. marinus*)	Genscan prediction ID or EST accession no.	Contig no.	Most similar gene [species] (accession no.)	*E*-value
TLR and their adaptor genes	TLR2a	GENSCAN00000027249	7641	Toll-like receptor 2 [*Sus scrofa*] (BAD90590)	2e-108
	TLR2b	GENSCAN00000120185	1179	TLR2 type2 [*G. gallus*] (BAB16842)	3e-121
	TLR2c	GENSCAN00000113984	1344	Toll-like receptor 6 [*Canis lupus familiaris*] (ACB41375)	2e-83
	TLR2d	GENSCAN00000096816	1344	Toll-like receptor b [*L. japonicum*] (BAE47506)	4e-50
	TLR14a	GENSCAN00000120396	35588	Toll-like receptor a [*L. japonicum*] (BAE47505)	0.0
	TLR14b	EB082826	4136	Toll-like receptor b [*L. japonicum*] (BAE47506)	0.0
	TLR14c	GENSCAN00000075432	9099	Toll-like receptor a [*L. japonicum*] (BAE47505)	7e-170
	TLR14d	GENSCAN00000133414	47492	Toll-like receptor 18 [*D. rerio*] (AAI62732)	2e-135
	TLR3	GENSCAN00000116058	18297	Toll-like receptor 3 [*Taeniopygia guttata*] (XP_002190888)	3e-134
	TLR5	GENSCAN00000136769	38231	TLRS5 [*T. rubripes*] (AAW69378)	4e-87
	TLR7/8a	GENSCAN00000159232	7539	Toll-like receptor 7 [*T. guttata*] (XP_002194911)	0.0
	TLR7/8b	Not predicted	30480	Similar to TLR8 [*Ornithorhynchus anatinus*] (XP_001515241)	2e-122
	TLR21a	GENSCAN00000145839	1528	Toll-like receptor 21 [*Ictalurus punctatus*] (ABF74622)	8e-175
	TLR21b	GENSCAN00000112026	15848	Toll-like receptor 21 [*I. punctatus*] (ABF74622)	2e-154
	TLR21c	GENSCAN00000006564	16741	Toll-like receptor 21 [*D. rerio*] (CAQ13807)	8e-146
	TLR22	GENSCAN00000052970	44660	Toll-like-receptor [*Oncorhynchus mykiss*] (CAF31506)	5e-92
	MyD88	gnl|ti|1309469868	8673	Similar to MyD88 [*Canis familiaris*] (XP_534223)	5e-47
	TICAM-1.1	GENSCAN00000029725	3393	Similar to TICAM-1 [*Monodelphis domestica*] (XP_001375102)	1e-27
	TICAM-1.2	GENSCAN00000011455	28649	TIR-containing adaptor molecule [*I. punctatus*] (ABD93874)	4e-22
	SARM	EC383618	12108	Sterile alpha and TIR motif containing 1 [*D. rerio*] (AAI63770)	2e-95
RLR and adaptor genes	RIG-I	CO546225	50584	RIG-I isoform 1 [*Pan troglodytes*] (XP_001156442)	5e-36
	LGP2	GENSCAN00000019608	2627	DHX58 [*Salmo salar*] (NP_001133649.1)	2e-13
	IPS-1	FD727562	427	Zgc:158392 [*D. rerio*] (AAI29222)	6e-11
TLR/RLR associated genes	LBP	DW024367	9431	MGC108117 protein [*X. tropicalis*] (NP_001015694.1)	2e-42
	IRAK1	GENSCAN00000011724	14150	IRAK1 protein [*Bos taurus*] (AAI08133.1)	5e-25
	IRAK3	GENSCAN00000072175	17420	novel protein similar to vertebrate IRAK3 [*D. rerio*] (CAQ13227.1)	1e-15
	IRAK4	FD717813	6289	IRAK4 [*Plecoglossus altivelis altivelis*] (BAH58736.1)	1e-22
	TRAF3	FD703125	45178	TRAF3 [*O. mykiss*] (NP_001118087.1)	1e-50
	TRAF6	GENSCAN00000012099	4693	TNF receptor-associated factor 6 [*Sus scrofa*] (NP_001098756.1)	3e-134
	TAK1	FD720776	2510	MAP kinase 7 [*X. tropicalis*] (NP_001093731.1)	2e-84
	TAB2	GENSCAN00000012731	19927	Similar to KIAA0733 [*M. domestica*] (XP_001370832.1)	7e-26
	TBK1	EB718759	13265	TANK-binding kinase 1 [*X. tropicalis*] (NP_001135652.1)	2e-21
	RIP1	gnl|ti|1229574012	1789	RIP1 [*Rattus norvegicus*] (NP_001100820.1)	5e-33
	CASP8	EG023282	11270	Caspase 8 [*G. gallus*] (NP_989923)	4e-14
	IKKα	GENSCAN00000034882	5202	IKKα [*T. guttata*] (XP_002186613.1)	3e-60
	IKKβ	GENSCAN00000073839	4708	Unnamed protein product [*Tetraodon nigroviridis*] (CAG09394.1)	3e-12
	IKKγ	CO548529	49136	Similar to IKKγ [*O. anatinus*] (XP_001505706.1)	5e-40
	IKKε	GENSCAN00000078948	48353	IKKε [*B. taurus*] (NP_001039810.1)	8e-16
	NAP1	GENSCAN00000070143	780	5-azacytidine induced 2 [*B. taurus*] (NP_001070473.1)	6e-13
	MKK6	GENSCAN00000036211	17299	Unnamed protein product [*T. nigroviridis*] (CAG03047.1)	2e-14
Transcription factor genes	IRF2	GENSCAN00000117845	17476	Similar to IRF2 isoform 1 [*Canis familiaris*] (XP_532847.2)	8e-47
	IRF4	GENSCAN00000134889	77775	Interferon regulatory factor 4 [*Equus caballus*] (XP_001487915.1)	6e-23
	IRF5	GENSCAN00000119547	65651	unnamed protein product [*T. nigroviridis*] (CAF90666.1)	2e-12
	IRF8	gnl|ti|1220653061	74379	Interferon regulatory factor 8 [*D. rerio*] (NP_001002622.1)	1e-11
	RELA	GENSCAN00000045445	69770	RELA isoform 1 [*H. sapiens*] (NP_068810.3)	3e-15
	NFκB1	CO548333	23299	Similar to NFκB1 p105 subunit [*D. rerio*] (XP_001339487.2)	1e-49
	ATF2	gnl|ti|1229751035	1160	Similar to ATF2 [*M. domestica*] (XP_001376719.1)	6e-09
	AP-1	GENSCAN00000027406	61254	unnamed protein product [*Coturnix coturnix*] (CAA33553.1)	2e-32
Antiviral genes	Mx	EE737404	23777	Mx protein [*Ctenopharyngodon idella*] (Q6TKS7)	2e-11
Not found	TLR4, TLR9, TLR13, TLR15, CD14, MD2, TIRAP, MDA5 IRAK2, TAB3, FADD, TANK, SINTBAD, MKK3, PKR, OAS1, Type I IFN (IFNα, β), TNF-α, IL-6, IL-12p40				

detected in the SMART browser. The size and number of the LRRs in each pmTLR were similar to the TLR counterparts of *T. rubripes* (Fig. 1).

3.2. Phylogenetic analysis of TLRs

To examine the relationships between vertebrate (human, mouse, chicken, xenopus, zebrafish, fugu, and lamprey) TLRs, a phylogenetic tree was constructed based upon the TLR sequences using the Clustal X and MEGA programs (Fig. 2). Phylogenetic analyses, which included the cytoplasmic TIR and extracellular LRR-regions, were performed as described previously (Ishii et al., 2007b). The constructed tree revealed the presence of several TLR subfamilies in pmTLRs: single clades were formed with TLR2a-b, TLR14a-c, TLR7/8a-b, TLR21a-c, and TLR24a-b. It is possible that each subfamily diverged through gene duplications that occurred after lampreys separated from the ancestor of common vertebrates.

There appeared to be a distinct cluster of pmTLR24, which formed a distinct clade from TLR2 and TLR1, 6, 10 in jawed vertebrates and the TLR14 subfamily. It is likely that the lamprey TLR2 subfamily expanded in a lamprey-specific manner. TLR14d was identified as an ortholog of TLR14 of jawed vertebrates with a high bootstrap value, forming a clade with the teleost TLR14 subfamily. In contrast, pmTLR14a-c showed a high similarity to ljTLR14a/b as indicated by their bootstrap values, suggesting that lamprey has two types of TLR14 with different primary sequences.

Although both pmTLR7/8a and 7/8b were mapped to the TLR7/8 cluster of jawed vertebrates, they separated in lamprey species independently of the divergence of TLR7 and TLR8 in jawed vertebrates. Whether pmTLR7/8a and 7/8b recognize nucleic acid

Please cite this article in press as: Kasamatsu, J., et al., Phylogenetic and expression analysis of lamprey toll-like receptors. Dev Comp Immunol (2010), doi:10.1016/j.dci.2010.03.004

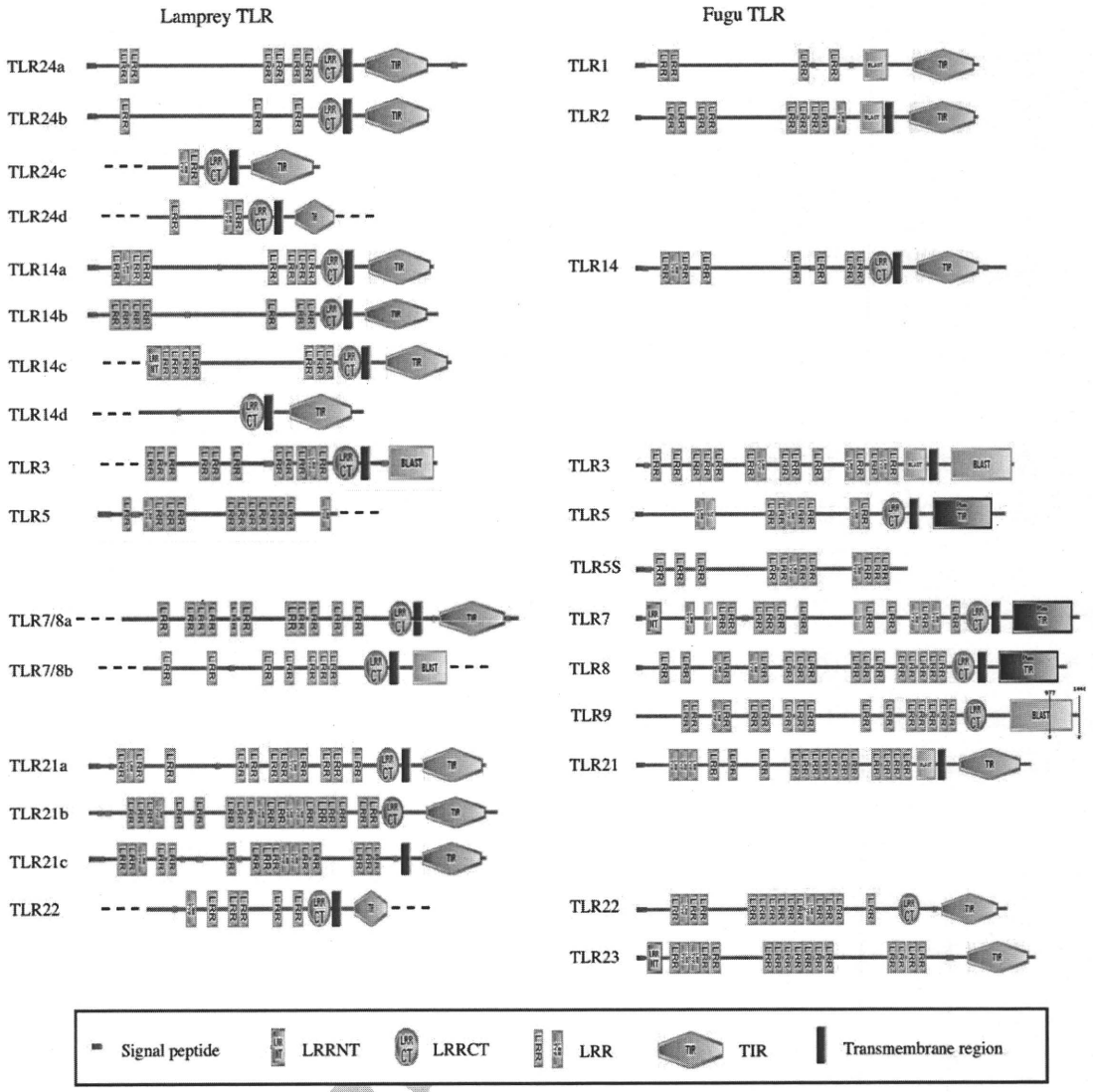

Fig. 1. Structures of the predicted *P. marinus* TLR proteins. Domains in the protein were predicted by the SMART program. LRRNTLRR, LRRCT transmembrane region and TIR domains are indicated in the picture. Left; lamprey TLRs. Right; fugu (*T. rubripes*) TLRs.

structures with different properties is presently unknown. The pmTLR21a-c genes were in the same cluster as the teleost TLR21 clade, while pmTLR22 was closest to the teleost TLR22 gene. There are only a single orthologs of TLR3 and TLR5 in lamprey (Fig. 2), which is consistent with a previous report on vertebrate TLR phylogenetic analysis (Kasahara, 2007). An examination of the tree suggests a rationale that lamprey TLRs correspond to the jawed vertebrate TLR orthologs (Fig. 2). The loci of these genes did not suggest that gene duplications simply occurred in the region resulting in two tandem sets of pmTLR14 and pmTLR24; the splitting of tandem genes may have occurred during the long history of the lamprey. The phylogenetic analysis based on their amino acid sequences reinforced the differential clustering of these TLR clades, which was likely rooted in the 'TLR big-bomb' which occurred ~600 million years ago (Ishii et al., 2007a).

3.3. Phylogenetic analyses of lamprey TLR adaptors

Human and mouse TLRs recruit the TIR-containing adaptors, MyD88 and TICAM-1 (Liew et al., 2005). For example, TLR2 recruits the complex adaptor TIRAP-MyD88, while TLR4 recruits two complex adaptors: TIRAP-MyD88 and TICAM-2–TICAM-1 (Takeda et al., 2003; Liew et al., 2005). The MyD88 pathway is dominant in mammals given that all TLRs, except for TLR3, bind MyD88. Only TLR3 and TLR4 link to the TICAM-1 pathway (Oshiumi et al., 2003b). The present lamprey TLR adaptor analyses allowed us to identify two TICAM-1 homologs, pmTICAM-1a and pmTICAM-1b (Fig. 3(A)), which resemble zebrafish TICAM-1, lacking the TRAF6-binding motif (Sullivan et al., 2007). The RHIM-like domain was conserved in pmTICAM-1b, as in zebrafish TICAM-1, but not in TICAM-1a. In the phylogenetic tree, pmTICAM-1a and b formed a clade with jawed vertebrates as well as mammalian TICAM-1 and 2 with high bootstrap values (Fig. 3(B)). In contrast, pmMyD88 and pmSARM belongs to their respective clades to form a single cluster with MyD88 and SARM of other jawed species with a high bootstrap support (Fig. 3(B)). From the observed amino acid identities between lamprey and jawed vertebrate TICAM genes, pmTICAM-1b was more similar to jawed vertebrate TICAM-1 than to TICAM-2, although pmTICAM-1a was nearly equidistant from all TICAM genes (Table 4). Therefore, these analyses indicate that pmTICAM-

Please cite this article in press as: Kasamatsu, J., et al., Phylogenetic and expression analysis of lamprey toll-like receptors. Dev Comp Immunol (2010), doi:10.1016/j.dci.2010.03.004

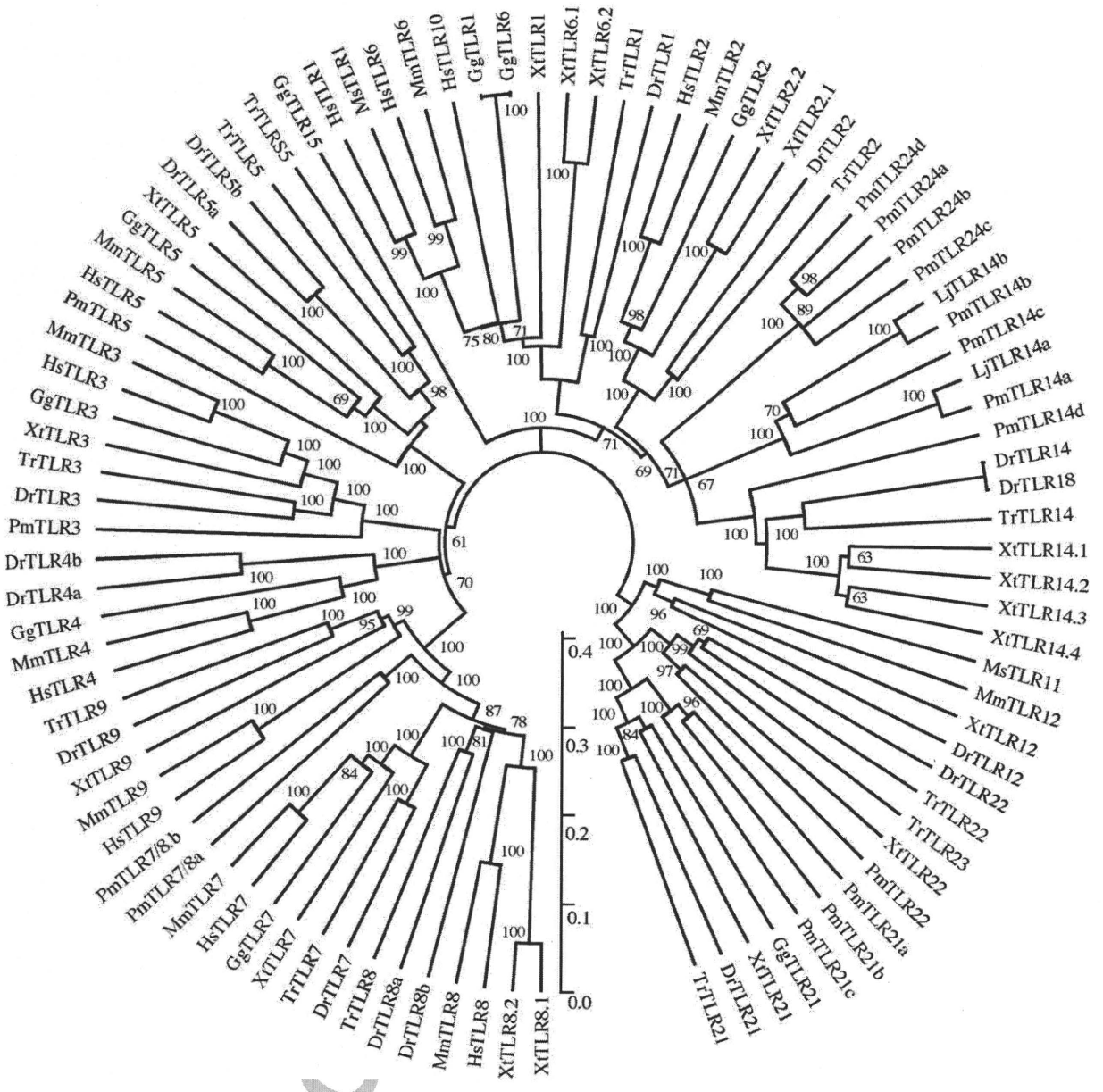

Fig. 2. Unrooted phylogenetic tree of vertebrate TLRs. The relationships were calculated on the basis of amino acid sequences of cytoplasmic TIR and extracellular LRR-regions. Bootstrap values (>60) are indicated. Hs; human (*Homo sapiens*), Mm; mouse (*Mus musculus*), Gg; chicken (*Gallus gallus*), Xt; frog (*Xenopus tropicalis*), Dr; zebrafish (*Danio rerio*), Tr; fugu (*T. rubripes*), Pm; Sea lamprey (*P. marinus*), Lj; Japanese lamprey (*L. japonicum*).

1b is the ortholog of jawed vertebrate TICAM-1 while pmTICAM-1a is either an ancestral or lamprey-specific TICAM gene.

3.4. Expression analysis of lamprey TLRs

RNA expressions of pmTLRs in several lamprey tissues were analyzed by RT-PCR. cDNA libraries were constructed from the eye, brain, gill, intestine, kidney, liver, muscle, skin, heart, and peripheral blood leukocytes (PBLs) from adult *L. japonicum* tissues. Each TLR primer set, except for pmTLR14a and b whose sequences were reported earlier (Ishii et al., 2007b), was derived from the nucleotide sequences of pmTLRs (Table 3). Almost all *L. japonicum* TLR cDNAs were successfully amplified using the sea lamprey primers, demonstrating that the sea lamprey and Japanese lamprey share similar TLR sets with very high homologies (Fig. 4). However, we could not amplify the TLR24c gene using any of the generated primer sets, nor could pmTLR24c be amplified using genomic DNA as a template. Further TBLASTN analysis using pmTLR24a as a query revealed that the N-terminal sequence of the TLR24c gene contained stop codon (data not shown), suggesting that ljTLR24c may in fact be a pseudogene, formed during the speciation of *P. marinus* and *L. japonicum* (Table 4).

The tissue distribution analysis indicated that every TLR mRNA was detected in each organ subjected to RT-PCR analyses (Fig. 4), although the level of expression differed among individual organs. All amplicons were sequenced and compared with sea lamprey TLR sequences by BLASTN analysis which revealed their partial nucleotide sequences were reasonably aligned with those predicted from the sea lamprey TLR genome (data not shown). Most lamprey TLR genes tended to be highly expressed in the gill, kid-

Please cite this article in press as: Kasamatsu, J., et al., Phylogenetic and expression analysis of lamprey toll-like receptors. Dev Comp Immunol (2010), doi:10.1016/j.dci.2010.03.004

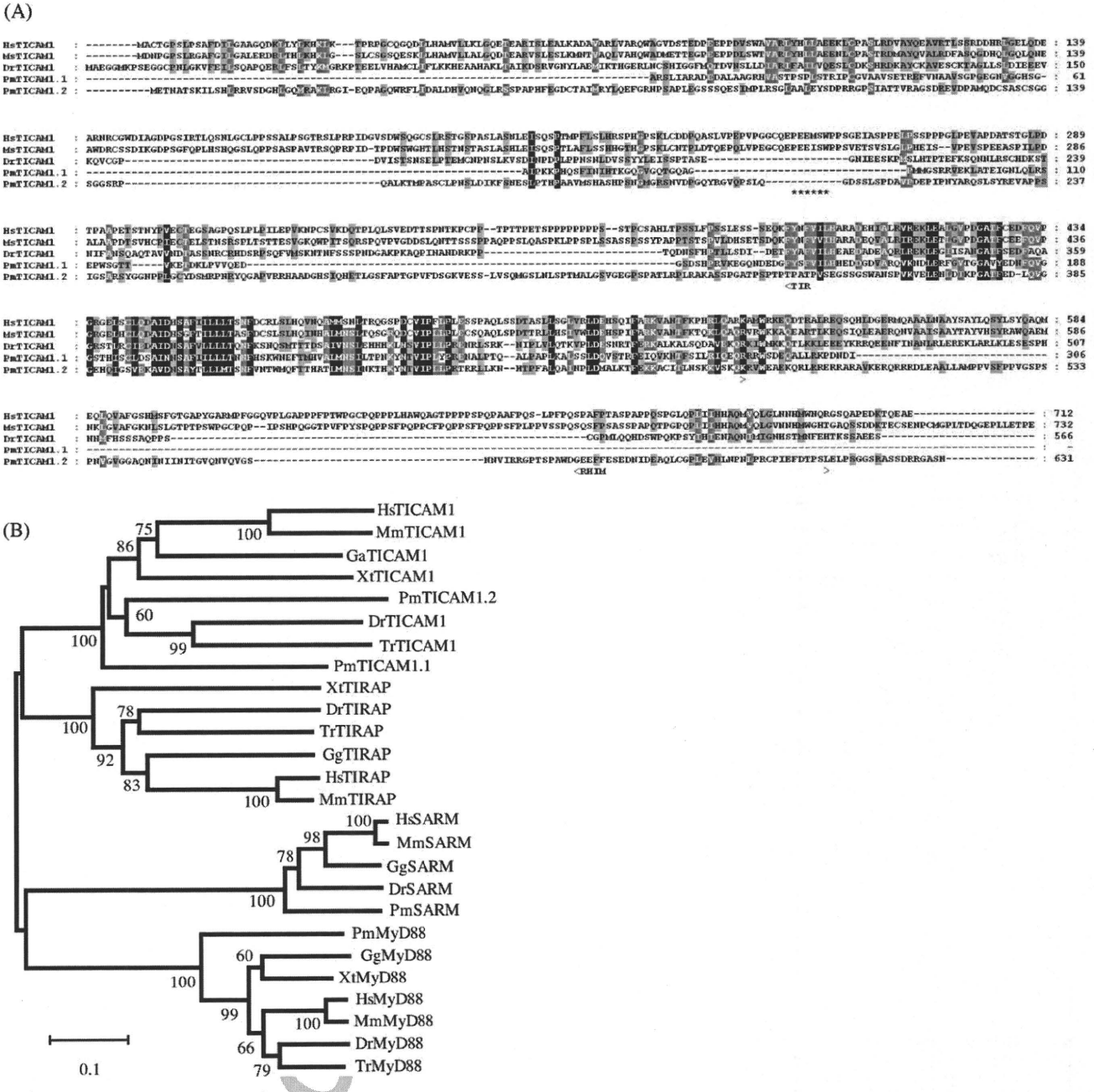

Fig. 3. (A) Alignment of vertebrate TICAM-1 sequences. An asterisk indicates the TRAF6-binding motif. Black shaded area, 100% identity; gray shaded area, 80–99% identity; light gray shaded area, 60–79% identity. (B) Unrooted phylogenetic tree of TIR-containing adaptors in vertebrates. The relationships were calculated on the basis of amino acid sequences of TIR domains. Bootstrap values (>60) are indicated. Hs; human (*H. sapiens*), Mm; mouse (*M. musculus*), Gg; chicken (*G. gallus*), Dr; zebrafish (*D. rerio*), Tr; fugu (*T. rubripes*), Pm; lamprey (*P. marinus*).

ney, and PBLs. Since these organs were rich in phagocytes and lymphocyte-like cells, TLRs may be dominantly expressed in the myeloid cells. Similarly, pmTICAM-1 adaptors were also expressed in the gill, kidney, and PBLs. Interestingly, pmTICAM-1a was predominantly expressed in the gill and PBLs, whereas pmTICAM-1b with the RHIM domain, was predominant in the kidney.

The ljTLR mRNA levels in PBLs were up- or down-regulated in response to polyI:C and heat-killed *E. coli*, which contain PAMPs (Fig. 5). ljTLR24a appeared to be transiently down-regulated while other ljTLRs were up-regulated 6 h after polyI:C stimulation. In contrast, *E. coli* stimulation tended to down-regulate mRNA levels of ljTLR3, 7/8b, 14b, and 21a. Thus, not only ljTLR3 but also ljTLR7/8a/b, 21a, 24b/c may be polyI:C-inducible genes and gene expression of most ljTLRs are controlled by exogenous microbial stimuli in lamprey.

4. Discussion

In this study, we annotated TLRs in the *P. marinus* genome using the latest assembled version of the Ensemble Lamprey Genome Browser database (released on August 2008), and determined their expression profiles by RT-PCR analyses within various organs in

Please cite this article in press as: Kasamatsu, J., et al., Phylogenetic and expression analysis of lamprey toll-like receptors. Dev Comp Immunol (2010), doi:10.1016/j.dci.2010.03.004

Table 3
Primers used in this study. The primers sets, excluding TLR14a and TLR14b, were constructed based on nucleotide sequences obtained from *P. marinus*.

Gene name	Forward primers (5′–3′)	Reverse primers (5′–3′)	PCR conditions (cycle and annealing temperature)
TLR2a	TGACTACCAATGCTCAAATCCAGAG	CCAGCTCAGGCAGGAGTTTC	35 cycles, 50 °C
TLR2b	CAACACACTACTGGGGATGAAACTAA	GTACCACAGCGCATCCAGGT	40 cycles, 50 °C
TLR2d	TCAATGCTCCAATCCAGAGAA	ATGATGTGGTGGCTGGGAAC	40 cycles, 50 °C
TLR14a	TCCTTGAGAGAGCTGTATCTGACG	AGTCCGAGTCCATGTGGCTGTAGG	40 cycles, 60 °C
TLR14b	TACATTGCACCCGAGTTGTACTCC	GTGGGCACCAGGGTGTTCTCCACC	45 cycles, 60 °C
TLR14c	TGGTCCCGACACTTGAGCAT	CGAGCGAGTCTTGGTTCTCC	40 cycles, 50 °C
TLR14d	CTACCGCTTCCACGCCTTC	GCTCGATGCTGTCGATGATG	35 cycles, 50 °C
TLR3	CGCTGTTCGTCCACTTTCA	GCTCCAGGTGTCTGCTCGTC	35 cycles, 50 °C
TLR5	CAGCATTGACCTCAGCCACA	GGCTATTGTTTGGGCTCCAC	40 cycles, 55 °C
TLR7/8a	TGCTACAATGCCCCTTACCC	GCCCTCAGCCAGTGCTTTT	35 cycles, 50 °C
TLR7/8b	GCTTCGACTGGTAGGGAATGG	CATCCCAAGGAATACGTGTCAG	35 cycles, 50 °C
TLR21a	GCGGTGTGCCAATCTTTCTC	TGGTTTCCACCCAGATCCAA	35 cycles, 50 °C
TLR21b	CCACGAGTTCCATGTGTCGT	CTTGAGGGTGATGAGGTTGCT	40 cycles, 50 °C
TLR21c	CCCCCAGTTGGAGAAAGAGG	ATGCGGTAGTAGGGCGACAG	35 cycles, 50 °C
TLR22	GTCTGCACCACCGCGACT	GCAGGTAGCTCCGCGTCA	35 cycles, 50 °C
MyD88	CACGTCCCGTAACAACAGCA	TGTCGGCGTAGCAGTAGCAG	33 cycles, 50 °C
TICAM1.1	GAGGGGCAGAATGATGAAGA	TTGTTCGGGGTTAGGATGGA	40 cycles, 50 °C
TICAM1.2	CTGGGCAGTACAGGGGTGTC	CGTCTCGTGCTGAATGCTGT	40 cycles, 50 °C
SARM	GCGATGAAGGAGAGCGTCA	CGCAGCAGTCCGTAGGTGT	35 cycles, 50 °C
EF1 alpha	CCATCGACATCTCTCTGTGGA	TAGTGCCGACGATGAGCTGCT	30 cycles, 60 °C

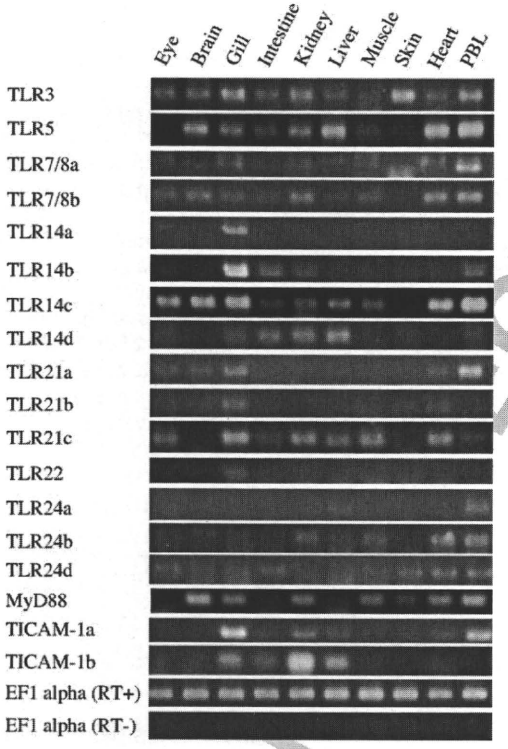

Fig. 4. Tissue expression profiles of *L. japonicum* TLR genes. All amplifications of the TLR cDNAs were performed by an identical PCR procedure. EF1 alpha was used as a positive control. No DNA was amplified by PCR regarding the EF1 alpha template from the non-reverse transcribed sample. Typical results were obtained using 30–45 PCR cycles.

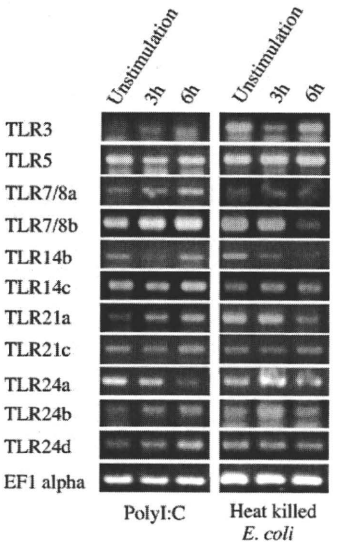

Fig. 5. Expression of blood cell ljTLRs in response to PAMP stimulation. Peripheral blood leukocytes were harvested from individuals of *L. japonicum*. Cells were separated into three groups: first group with no stimulation (unstimulation), second group with 3 h stimulation (3 h) and third group with 6 h stimulation. PolyI:C (10 μg/ml) and heat killed *E. coli* (3×10^7 cell/ml) were used as stimulators as indicated. EF1 was used as a positive control.

adult lampreys of *L. japonicum*. The overall features of the lamprey TLR system appear to resemble those of teleosts living in water in that they commonly express incomplete M-type TLRs and have more sophisticated F-type TLRs than land animals. The levels of ljTLRs in lamprey PBLs are regulated by PAMP stimuli as observed in mouse macrophages.

The prominent characteristics of the lamprey TLR system as compared to the teleost TLR system, are outlined below. We found three types of TLRs from the TLR2 subfamily in the lamprey, which correspond to TLR24 (pmTLR2a-d), TLR14 (pmTLR14a-c), and the ortholog of jawed vertebrate TLR14 (TLR14d), forming clearly distinct clusters in the phylogenetic tree. The TLR2 subfamily consists of multiple members displaying wide variability across animal species (Leulier and Lemaitre, 2008). Our past studies have shown that members of the chicken and amphibian TLR2 subfamily arose by lineage-specific duplication events (Ishii et al., 2007a; Higuchi et al., 2008). In combination with TLR2, human and mouse TLR1 and TLR6 facilitate the discrimination between triacylated and diacylated bacterial lipoproteins, respectively (Takeda et al., 2003). In contrast, chicken TLR2 proteins (chTLR1-1,2 and chTLR2-1,2) recognize bacterial lipoproteins and peptidoglycan in a different manner than human and mice (Higuchi et al., 2008). These studies suggest that divergence of the TLR2 subfamily seems to have developed by

Please cite this article in press as: Kasamatsu, J., et al., Phylogenetic and expression analysis of lamprey toll-like receptors. Dev Comp Immunol (2010), doi:10.1016/j.dci.2010.03.004

Table 4
Amino acid identities between human, mouse, zebrafish, and lamprey TICAM genes. Hs; human (*H. sapiens*), Mm; mouse (*M. musculus*), Dr; zebrafish (*D. rerio*), Pm; lamprey (*P. marinus*).

	HsTICAM-1	MmTICAM-1	DrTICAM-1	HsTICAM-2	MmTICAM-2	PmTICAM-1b
PmTICAM-1a	15.6%	14.0%	18.8%	18.2%	15.5%	18.9%
PmTICAM-1b	19.8%	19.3%	18.5%	9.4%	9.1%	–

gene duplication events and have allowed animals to specifically cope with pathogens sharing living environment with them.

Similarly, we also identified two TLR7/8 and three TLR21 genes in the lamprey genome. TLR3, 7, and 8, and teleost TLR22 recognize foreign RNA, while TLR9 and chicken TLR21 recognize unmethylated CpG DNAs (Matsuo et al., 2008; Brownlie et al., 2009). Therefore, our analysis indicates that lamprey has developed not only the TLR2 subfamily, but also other TLR proteins which recognize nucleic acids. This then begs the question: what was the original vertebrate TLR system? Table 5 shows a summary of the TLR repertoire present in deuterostomes. The TLR2 subfamily, TLR3, TLR5, TLR7/8, and TLR21/22 are essentially conserved in the lamprey and teleosts, suggesting that lampreys and jawed vertebrates conform to the same TLR family with hybrid M- and F-type TLRs, which may represent the origin of the TLR repertoire in vertebrates.

The vertebrate TLR phylogenetic tree in Fig. 2 appears as a star-like tree (Roach et al., 2005), and such a phylogram shape suggests that each TLR family was generated at the same time, which we termed the "TLR big-bomb". While the sea urchin and amphioxus possess approximately 200 (Hibino et al., 2006; Rast et al., 2006) and 50 TLRs (Holland et al., 2008; Huang et al., 2008), respectively, *C. intestinalis* has only 2 functional TLRs (Sasaki et al., 2009) identified from their genomes. In phylogenetic analyses of these studies, invertebrate TLRs did not clearly belong to vertebrate M- and F-type TLRs (Hibino et al., 2006; Holland et al., 2008; Huang et al., 2008; Sasaki et al., 2009). Therefore, M- and F-type TLRs may have arisen together with the origin of vertebrates. Interestingly, despite having only two TLRs, *C. intestinalis* can recognize a broad spectrum of PAMPs (Sasaki et al., 2009), indicating these unique invertebrate TLRs may have been an alternative origin of mammalian TLRs. In other words, vertebrate TLR proteins did not always recognize just one specific PAMP, but were able to recognize several PAMPs using a single type of M-type TLR (Sasaki et al., 2009). The gain or loss of these TLRs may have occurred during the evolution of vertebrates, although it is also possible that differential environmental factors promoted TLR divergence for animals to survive against microbial milieu, which although interesting to speculate, is beyond the scope of this analysis.

Our database analyses failed to identify orthologs of TLR4, 9 and 15, nor the TLR4-related genes, CD14, MD-2, and TIRAP in the Pre-Ensemble Lamprey Genome Browser database (Table 2). Absence of orthologs of CD14, MD-2 and TIRAP in lamprey may reflect the lack of a TLR4 system in lamprey as well as in teleosts and amphibia (Ishii et al., 2007a). It has long been established that teleosts are resistant to toxic effect of LPS. Recent study shows that zebrafish TLR4 acts as a negative regulator for NF-κB-signaling pathway, not for recognition of LPS (Sepulcre et al., 2009). Hence, these observations indicate that first the TLR4 gene arose in jawed vertebrates as a negative regulator of NF-κB-signaling pathway, and then it may have gained the function of LPS recognition with CD14 and MD-2 in an ancestor of amniota.

Additionally, we identified two TICAM genes, named TICAM-1a and b, in the lamprey genome. A previous study indicated that mammalian TICAM-1 and 2 genes resulted from two rounds of genome duplication, termed the 2R hypothesis, in early vertebrate evolution (Sullivan et al., 2007). In this hypothesis, one of the ancestral TICAM genes was lost after the first round of genome duplication, while after the second genome duplication, the TICAM-1 and 2 genes appeared. Although the timing of the genome duplications is still unclear (Kasahara, 2007; Panopoulou and Poustka, 2005), preliminary analyses of *HOX* gene clusters indicates the first round of genome duplication occurred in a common ancestor of jawed and jawless vertebrates (Irvine et al., 2002). In our analysis, pmTICAM-1b was identified as the

Table 5
TLR repertoires in deuterostomes.

	Human	Mouse	Chicken	Frog	Zebrafish	Fugu	Lamprey	Ascidian	Amphixus	Sea urchin
TLR1	+	+	+	+	+	+	–			
TLR2	+	+	+	+	+	+	–			
TLR3	+	+	+	+	+	+	+			
TLR4	+	+	+	+	+	–	–			
TLR5	+	+	+	+	+	+	+			
TLR6	+	+	*psd*	–	–	–	–			
TLR7	+	+	+	+	+	+	+			
TLR8	+	+	+	+	+	+	+	~2?	~36?	~300?
TLR9	+	+	–	+	+	+	–			
TLR10	+	*psd*	–	–	–	–	–			
TLR12 (TLR11)	–	+	–	+	–	+	–			
TLR13	–	+	–	+	–	–	–			
TLR14 (TLR15)	–	–	+	+	+	+	+			
TLR21	–	–	–	+	+	+	+			
TLR22 (TLR23)	–	–	–	+	+	+	+			
TLR24	–	–	–	–	–	–	+			
MyD88	+	+	+	+	+	+	+	+	+	+
TICAM	+	+	+	+	+	+	+	–	+	–
RIG-I	+	+	+	+	+	+	+	–	+	–
MDA5	+	+	+	+	+	+	–	–	–	+
IPS-1	+	+	+	+	+	+	+	–	–	+
IRF3	+	+	–	+	+	+	–	–	–	–
IRF7	+	+	+	+	+	+	–	–	–	–
IFN	+	+	+	+	+	+	–	–	–	–

+; exists, –; does not exist, *psd*; pseudogene.

Please cite this article in press as: Kasamatsu, J., et al., Phylogenetic and expression analysis of lamprey toll-like receptors. Dev Comp Immunol (2010), doi:10.1016/j.dci.2010.03.004

ortholog of jawed vertebrate TICAM-1, whereas pmTICAM-1a did not show clear similarity to either TICAM-1 or TICAM-2. It is possible that pmTICAM-1a represents an ancestral gene of TICAM-2 that occurred during the first genome duplication event without gene loss. There are many TLRs binding to TICAM-1 in teleosts (Matsuo et al., 2008; Baoprasertkul et al., 2006), and TICAM-1a and b might have diverged due to the necessity for differential signaling of TICAM-associated TLRs in the lamprey.

Although the orthologs of nucleic acid-recognizing TLRs were predicted in the genome and confirmed by RT-PCR, no genes related to type I IFN induction except for the antiviral Mx gene were identified in the lamprey. While RIG-I/IPS-1, TBK1/IKKε and IRF-2, 4, 5, and 8 are present, genes corresponding to IRF-1, IRF-3, IRF-7, and type I IFN are not conserved in the lamprey genome (Table 2). The presence of the IFN-inducing pathway in lamprey is controversial as whole genome sequencing projects in ectoderms and primitive chordates, including sea urchin, amphioxus, and ascidian, have revealed the lack of type I IFN and its essential transcription factors, IRF-3 and IRF-7 (Table 5) (Hibino et al., 2006; Holland et al., 2008; Huang et al., 2008; Sasaki et al., 2009). Therefore, IFN-inducing pathway would be completed in a common ancestor of jawed vertebrates. Type I IFN plays a critical role in facilitating TCR-MHC-mediated lymphocyte activation of the acquired immune response in mammals. Although lamprey has many orthologs of jawed vertebrate TLRs and TLR-associated signaling molecules, it does not have MHC or authentic TCR/BCR.

Recent findings have indicated that lamprey possesses a unique acquired immune system involving variable lymphocyte receptors (VLRs) and the lymphoid system (Pancer and Cooper, 2006; Pancer et al., 2004; Flajnik, 2007; Kasahara et al., 2008). In agnathans, which includes lamprey and hagfish, clonally diversed receptors are generated by the assembly of genes for VLRA and VLRB, which are comprised of leucine-rich repeat (LRR) subunits and an invariant membrane-proximal stalk region (Pancer and Cooper, 2006; Pancer et al., 2005). Interestingly, the variable VLRA and VLRB products consist of a number of LRR motifs representing soluble forms and membrane-bound forms, respectively (Guo et al., 2009). Hence, the VLR-expressing lymphocytes are similar to authentic B and T cells in jawed vertebrates. Our study indicates that VLR-based acquired immunity may be regulated by TLRs with IFN-independent systems in jawless vertebrates. Functional analyses of lamprey TLRs need to be conducted in the future.

We can speculate from the current results that both water and land vertebrates possess common TLR proteins that may participate in the recognition of common PAMPs (Hirono et al., 2004). Indeed, lamprey also expresses a set of TLRs as in fish despite their evolutionary separation approximately 500 million years ago. The present results allow us to surmise that the TLR orthologs in lamprey and mammals recognize common PAMPs for host defense. The TLR system may serve to protect lampreys from infections despite the fact that their acquired immune system is modally different.

Acknowledgements

We are grateful to our laboratory members for invaluable discussions. This work was supported in part by Grants-in-Aid from the Ministry of Education, Science, and Culture (Specified Project for Advanced Research) of Japan and in part by the Program of Founding Research Centers for Emerging and Reemerging Infectious Diseases, MEXT. The supports by the Mitsubishi Foundation (TS), Takeda Foundation (TS) and Uehara memorial Foundation (MM) were gratefully acknowledged.

References

Baoprasertkul, P., Peatman, E., Somridhivej, B., Liu, Z., 2006. Toll-like receptor 3 and TICAM genes in catfish: species-specific expression profiles following infection with *Edwardsiella ictaluri*. Immunogenetics 58, 817–830.
Boyd, A., Philbin, V., Smith, A., 2007. Conserved and distinct aspects of the avian toll-like receptor (TLR) system: implications for transmission and control of bird-borne zoonoses. Biochem. Soc. Trans. 35, 1504–1507.
Brownlie, R., Zhu, J., Allan, B., Mutwiri, G., Babiuk, L., Potter, A., et al., 2009. Chicken TLR21 acts as a functional homologue to mammalian TLR9 in the recognition of CpG oligodeoxynucleotides. Mol. Immunol. 46, 3163–3170.
Flajnik, M., 2007. Immunogenetics: alternative strategies in adaptive immunity and the rise of comparative immunogenomics. Curr. Opin. Immunol. 19, 522–525.
Flajnik, M., Kasahara, M., 2001. Comparative genomics of the MHC: glimpses into the evolution of the adaptive immune system. Immunity 15, 351–362.
Guo, P., Hirano, M., Herrin, B., Li, J., Yu, C., Sadlonova, A., et al., 2009. Dual nature of the adaptive immune system in lampreys. Nature 459, 796–801.
Hibino, T., Loza-Coll, M., Messier, C., Majeske, A., Cohen, A., Terwilliger, D., et al., 2006. The immune gene repertoire encoded in the purple sea urchin genome. Dev. Biol. 300, 349–365.
Higuchi, M., Matsuo, A., Shingai, M., Shida, K., Ishii, A., Funami, K., et al., 2008. Combinational recognition of bacterial lipoproteins and peptidoglycan by chicken toll-like receptor 2 subfamily. Dev. Comp. Immunol. 32, 147–155.
Hirono, I., Takami, M., Miyata, M., Miyazaki, T., Han, H., Takano, T., et al., 2004. Characterization of gene structure and expression of two toll-like receptors from Japanese flounder, *Paralichthys olivaceus*. Immunogenetics 56, 38–46.
Holland, L., Albalat, R., Azumi, K., Benito-Gutiérrez, E., Blow, M., Bronner-Fraser, M., et al., 2008. The amphioxus genome illuminates vertebrate origins and cephalochordate biology. Genome Res. 18, 1100–1111.
Huang, S., Yuan, S., Guo, L., Yu, Y., Li, J., Wu, T., et al., 2008. Genomic analysis of the immune gene repertoire of amphioxus reveals extraordinary innate complexity and diversity. Genome Res. 18, 1112–1126.
Irvine, S., Carr, J., Bailey, W., Kawasaki, K., Shimizu, N., Amemiya, C., et al., 2002. Genomic analysis of Hox clusters in the sea lamprey *Petromyzon marinus*. J. Exp. Zool. 294, 47–62.
Ishii, A., Kawasaki, M., Matsumoto, M., Tochinai, S., Seya, T., 2007a. Phylogenetic and expression analysis of amphibian Xenopus toll-like receptors. Immunogenetics 59, 281–293.
Ishii, A., Matsuo, A., Sawa, H., Tsujita, T., Shida, K., Matsumoto, M., et al., 2007b. Lamprey TLRs with properties distinct from those of the variable lymphocyte receptors. J. Immunol. 178, 397–406.
Kasahara, M., 2007. The 2R hypothesis: an update. Curr. Opin. Immunol. 19, 547–552.
Kasahara, M., Kasamatsu, J., Sutoh, Y., 2008. Two types of antigen receptor systems in vertebrates. Zoolog. Sci. 25, 969–975.
Larkin, M., Blackshields, G., Brown, N., Chenna, R., McGettigan, P., McWilliam, H., et al., 2007. Clustal W and Clustal X version 2.0. Bioinformatics 23, 2947–2948.
Lemaitre, B., Nicolas, E., Michaut, L., Reichhart, J., Hoffmann, J., 1996. The dorsoventral regulatory gene cassette spätzle/Toll/cactus controls the potent antifungal response in Drosophila adults. Cell 86, 973–983.
Leulier, F., Lemaitre, B., 2008. Toll-like receptors – taking an evolutionary approach. Nat. Rev. Genet. 9, 165–178.
Liew, F., Xu, D., Brint, E., O'Neill, L., 2005. Negative regulation of toll-like receptor-mediated immune responses. Nat. Rev. Immunol. 5, 446–458.
Litman, G., Anderson, M., Rast, J., 1999. Evolution of antigen binding receptors. Annu. Rev. Immunol. 17, 109–147.
Matsuo, A., Oshiumi, H., Tsujita, T., Mitani, H., Kasai, H., Yoshimizu, M., et al., 2008. Teleost TLR22 recognizes RNA duplex to induce IFN and protect cells from birnaviruses. J. Immunol. 181, 3474–3485.
Medzhitov, R., Preston-Hurlburt, P., Janeway, C.J., 1997. A human homologue of the Drosophila toll protein signals activation of adaptive immunity. Nature 388, 394–397.
Oshiumi, H., Tsujita, T., Shida, K., Matsumoto, M., Ikeo, K., Seya, T., 2003a. Prediction of the prototype of the human toll-like receptor gene family from the pufferfish Fugu rubripes, genome. Immunogenetics 54, 791–800.
Oshiumi, H., Sasai, M., Shida, K., Fujita, T., Matsumoto, M., Seya, T., 2003b. TIR-containing adapter molecule (TICAM)-2, a bridging adapter recruiting to toll-like receptor 4 TICAM-1 that induces interferon-beta. J. Biol. Chem. 278, 49751–49762.
Oshiumi, H., Matsuo, A., Matsumoto, M., Seya, T., 2008. Pan-vertebrate toll-like receptors during evolution. Curr. Genomics 9, 488–493.
Pancer, Z., Cooper, M., 2006. The evolution of adaptive immunity. Annu. Rev. Immunol. 24, 497–518.
Pancer, Z., Amemiya, C., Ehrhardt, G., Ceitlin, J., Gartland, G., Cooper, M., 2004. Somatic diversification of variable lymphocyte receptors in the agnathan sea lamprey. Nature 430, 174–180.
Pancer, Z., Saha, N., Kasamatsu, J., Suzuki, T., Amemiya, C., Kasahara, M., et al., 2005. Variable lymphocyte receptors in hagfish. Proc. Natl. Acad. Sci. U.S.A. 102, 9224–9229.
Panopoulou, G., Poustka, A., 2005. Timing and mechanism of ancient vertebrate genome duplications – the adventure of a hypothesis. Trends Genet. 21, 559–567.
Rast, J., Smith, L., Loza-Coll, M., Hibino, T., Litman, G., 2006. Genomic insights into the immune system of the sea urchin. Science 314, 952–956.
Roach, J., Glusman, G., Rowen, L., Kaur, A., Purcell, M., Smith, K., et al., 2005. The evolution of vertebrate toll-like receptors. Proc. Natl. Acad. Sci. U.S.A. 102, 9577–9582.

Please cite this article in press as: Kasamatsu, J., et al., Phylogenetic and expression analysis of lamprey toll-like receptors. Dev Comp Immunol (2010), doi:10.1016/j.dci.2010.03.004

Sasaki, N., Ogasawara, M., Sekiguchi, T., Kusumoto, S., Satake, H., 2009. Toll-like receptors of the ascidian *Ciona intestinalis*: prototypes with hybrid functionalities of vertebrate toll-like receptors. J. Biol. Chem. 284, 27336–27343.

Sepulcre, M., Alcaraz-Pérez, F., López-Muñoz, A., Roca, F., Meseguer, J., Cayuela, M., et al., 2009. Evolution of lipopolysaccharide (LPS) recognition and signaling: fish TLR4 does not recognize LPS and negatively regulates NF-kappaB activation. J. Immunol. 182, 1836–1845.

Seya, T., Matsumoto, M., 2009. The extrinsic RNA-sensing pathway for adjuvant immunotherapy of cancer. Cancer Immunol. Immunother. 58, 1175–1184.

Seya, T., Matsumoto, M., Ebihara, T., Oshiumi, H., 2009. Functional evolution of the TICAM-1 pathway for extrinsic RNA sensing. Immunol. Rev. 227, 44–53.

Sullivan, C., Postlethwait, J., Lage, C., Millard, P., Kim, C., 2007. Evidence for evolving toll-IL-1 receptor-containing adaptor molecule function in vertebrates. J. Immunol. 178, 4517–4527.

Takeda, K., Kaisho, T., Akira, S., 2003. Toll-like receptors. Annu. Rev. Immunol. 21, 335–376.

Tamura, K., Dudley, J., Nei, M., Kumar, S., 2007. MEGA4: molecular evolutionary genetics analysis (MEGA) software version 4.0. Mol. Biol. Evol. 24, 1596–1599.

Please cite this article in press as: Kasamatsu, J., et al., Phylogenetic and expression analysis of lamprey toll-like receptors. Dev Comp Immunol (2010), doi:10.1016/j.dci.2010.03.004

The Peptide Sequence of Diacyl Lipopeptides Determines Dendritic Cell TLR2-Mediated NK Activation

Masahiro Azuma[1☯], Ryoko Sawahata[1☯], Yuusuke Akao[1☯¤a], Takashi Ebihara[1¤b], Sayuri Yamazaki[1], Misako Matsumoto[1], Masahito Hashimoto[2], Koichi Fukase[3], Yukari Fujimoto[3], Tsukasa Seya[1]*

1 Department of Microbiology and Immunology, Graduate School of Medicine, Hokkaido University, Sapporo, Japan, **2** Department of Nanostructure and Advanced Materials, Kagoshima University, Kagoshima, Japan, **3** Department of Chemistry, Graduate School of Science, Osaka University, Toyonaka, Japan

Abstract

Natural killer (NK) cells are lymphocyte effectors that are activated to control certain microbial infections and tumors. Many NK-activating and regulating receptors are involved in regulating NK cell function. In addition, activation of naïve NK cells is fundamentally triggered by cytokines or myeloid dendritic cells (mDC) in various modes. In this study, we synthesized 16 S-[2,3-bis(palmitoyl)propyl]cysteine (Pam2Cys) lipopeptides with sequences designed from lipoproteins of *Staphylococcus aureus*, and assessed their functional properties using mouse (C57BL/6) bone marrow-derived DC (BMDC) and NK cells. NK cell activation was evaluated by three criteria: IFN-γ production, up-regulation of NK activation markers and cytokines, and NK target (B16D8 cell) cytotoxicity. The diacylated lipopeptides acted as TLR2 ligands, inducing up-regulation of CD25/CD69/CD86, IL-6, and IL-12p40, which represent maturation of BMDC. Strikingly, the Pam2Cys lipopeptides induced mouse NK cell activation based on these criteria. Cell-cell contact by Pam2Cys peptide-stimulated BMDC and NK cells rather than soluble mediators released by stimulated BMDC induced activation of NK cells. For most lipopeptides, the BMDC TLR2/MyD88 pathway was responsible for driving NK activation, while some slightly induced direct activation of NK cells via the TLR2/MyD88 pathway in NK cells. The potential for NK activation was critically regulated by the peptide primary sequence. Hydrophobic or proline-containing sequences proximal to the N-terminal lipid moiety interfered with the ability of lipopeptides to induce BMDC-mediated NK activation. This mode of NK activation is distinctly different from that induced by polyI:C, which is closely associated with type I IFN-inducing pathways of BMDC. These results imply that the MyD88 pathway of BMDC governs an alternative NK-activating pathway in which the peptide sequence of TLR2-agonistic lipopeptides critically affects the potential for NK activation.

Citation: Azuma M, Sawahata R, Akao Y, Ebihara T, Yamazaki S, et al. (2010) The Peptide Sequence of Diacyl Lipopeptides Determines Dendritic Cell TLR2-Mediated NK Activation. PLoS ONE 5(9): e12550. doi:10.1371/journal.pone.0012550

Editor: Jacques Zimmer, Centre de Recherche Public de la Santé, Luxembourg

Received June 10, 2010; **Accepted** July 30, 2010; **Published** September 2, 2010

Funding: This work was supported in part by Grants-in-Aid from the Ministry of Education, Science, and Culture (Specified Project for Advanced Research) and the Ministry of Health, Labor, and Welfare of Japan, and by the Yakult and Waxmann Foundations. Financial support by the Sapporo Biocluster "Bio-S" the Knowledge Cluster Initiative of the MEXT, is gratefully acknowledged. The funders had no role in study design, data collection and analysis, decision to publish, or preparation of the manuscript.

Competing Interests: The authors have declared that no competing interests exist.

* E-mail: seya-tu@pop.med.hokudai.ac.jp

☯ These authors contributed equally to this work.

¤a Current address: Yakult Central Institute for Microbiological Research, Kunitachi, Tokyo, Japan
¤b Current address: Howard Hughes Medical Institute, Washington University School of Medicine, St. Louis, Missouri, United States of America

Introduction

Natural killer (NK) cells function in early defense against various pathogens. Microbial pattern molecules activate NK cells by stimulating pattern-recognition receptors (PRRs) in NK cells or myeloid dendritic cells (mDC) [1]. mDC-mediated NK activation occurs secondary to mDC maturation, and is competent to induce NK-activating cytokines or mDC membrane molecules to facilitate reciprocal activation of mDC and NK cells [1,2]. Toll-like receptors (TLRs) and cytoplasmic pattern sensors are PRRs that may be associated with mDC-mediated NK activation [1,3]. In mDC, TLR3 and cytoplasmic sensors, RIG-I/MDA5 usually participate in driving NK activation in response to double-stranded (ds)RNA [4–6].

Staphylococcus aureus, a versatile Gram-positive pathogen, is reported to activate NK cells during infection [7]. *S. aureus* cell wall components including peptidoglycan, lipoproteins, and alanylated lipoteichoic acid, are inflammation inducers, and provoke the activation of host immune cells [8]. *S. aureus* cell wall pattern molecules are mainly recognized by cell-surface TLR2 and cytoplasmic nucleotide-binding oligomerization domain 2 (Nod2) in host cells, which signal the presence of bacterial infection. Mice lacking TLR2 or the adaptor protein MyD88 are highly susceptible to *S. aureus* infection [9]. The molecular basis by which *S. aureus* activates host immunity has been investigated, and lipoprotein, rather than lipoteichoic acid, is the main trigger of immune stimulation [10] that preferentially activates TLR2 in mouse cells. TLR2/MyD88 determines the pathway for activation of macrophages in mice [11]. Lipoprotein also activates TLR2 in human cells [12,13].

The functional properties of *S. aureus* lipopeptides have been investigated in gene-disrupted mice [9,14,15]. TLR2, in concert with TLR1 or TLR6, is involved in their recognition [16,17]. Two adaptor proteins, TIRAP and MyD88, deliver TLR2 signals that

activate NF-κB [18,19], which functions in cytokine induction. These studies were mainly performed in mouse macrophages, and results were essentially consistent with other biochemical studies using macrophages [20,21]. Nonetheless, more complicated regulation may occur in other immune-related cells, including mDCs. Recent studies suggested that in mDCs, TLR2 and MyD88 are involved in NK activation that is provoked by bacterial pattern molecules [22,23]. Our previous results also inferred that bacterial lipoproteins act as TLR2 agonists in mDC-driven NK activation [24].

In mDCs, a subset of the antigen-presenting cells, the two major arms of the innate immune signaling pathway, the MyD88 and TICAM-1 (TRIF) pathways, function in the TLR signaling [18,19]. In addition, cytokines including IL-12, IL-15 and IFN-α/β, as well as DC-NK contact are involved in NK cell activation [25,26]. TLR3 is a sensor of dsRNA and induces mDC maturation via TICAM-1 [4,25]. A characteristic feature of TLR3-TICAM-1-mediated mDC maturation is liberation of IL-12, and, independent of IL-12, drives NK cell activation [4]. On the other hand, what factors participate in TLR2-MyD88-mediated mDC maturation to drive NK activation remains largely unknown.

We identified lipopeptides from Triton X-114-solubilized *S. aureus* cells [27,28]. Since *S. aureus* lacks lipoprotein N-acyltransferase, these lipoproteins are predicted to be S-[2,3-bis(palmitoyl)-propyl]cysteines (Pam2Cys) [29]. Their diacylated structure was confirmed by MS/MS spectrometry [28]. We annotated these lipoproteins by function, which largely depends on their protein sequence [30]. Based on these results, we chemically synthesized 16 Pam2Cys lipopeptides of 6–18 amino acids (a.a.) [30]. They possessed TLR2 agonistic activity, but varied in their functional potential to activate NF-κB and liberate TNF-α from human PBMC [30], yet their NK activation potential has not been determined.

This study shows that naïve NK cells are usually in a resting state, and bacterial lipoproteins trigger mDC-mediated NK activation in response to TLR2-derived cellular events. We found that mDC maturation and NK activation are strongly modulated by the amino acid (a. a.) sequence of TLR2 agonistic lipopeptides.

Results

Cytokines liberated from BMDC in response to Pam2 peptides

We synthesized 16 Pam2Cys-containing lipopeptides using *S. aureus* lipoproteins as a reference [30], and designated them Pam2Cys1-Pam2Cys16 (Table 1). Included as positive controls were the diacyl lipopeptides Pam2CSK4 [31], designated as Pam2CSK19 in this study, and its derivatives Pam2CSK (Pam2Cys17), and Pam2CSK2 (Pam2Cys18). Pam2Cys17 was used as a negative control, since this diacyl lipopeptide has virtually no cytokine-inducing activity (Fig. 1). ELAM-luciferase reporter assays were used to assess the NF-κB activation potential of these lipopeptides at 10–500 nM, and a representative result for 100 nM is in Figure 1A. Pam2Cys18 and 19 showed high reporter activity, but Pam2Cys17 did not (Fig. 1A). A series longer than 3 a. a were essential for TLR2 stimulation. The level of TNF-α liberated from mouse BMDC was largely comparable with that induced by human PBMC (Table 1). Pam2Cys4, Pam2Cys13, Pam2Cys15 and Pam2Cys16 exhibited relatively low NF-kB activation and TNF-α production (Table 1, Fig. 1A).

IL-6 and IL-12p40 levels were determined by ELISA using the supernatant of the media from bone marrow-derived DC (BMDC) culture with the lipopeptides for 24 h. The cytokines were detected at high levels in the cultures with lipopeptides, with the exception of Pam2Cys17, Pam2Cys13, and Pam2Cys16 (Fig. 1B,C). The cytokine contents of wells with BMDCs stimulated with Pam2Cys13 and Pam2Cys16 were as low as the control Pam2Cys17.

Table 1. Pam2 lipopeptides used for this study.

No.	Lipid	Amino acid sequence	TNF-α*
Pam2Cys1	Pam2	CANTRHSESDK	++
Pam2Cys2	Pam2	CGTGGKQSSDK	++
Pam2Cys3	Pam2	CGNGNKSGSDD	++
Pam2Cys4	Pam2	CSNIEIFNAKG	+/−
Pam2Cys5	Pam2	CTTDKKEIKAY	+++
Pam2Cys6	Pam2	CSFGGNHKLSS	++
Pam2Cys7	Pam2	CGSQNLAPLEE	+++
Pam2Cys8	Pam2	CGQDSDQQKDG	+++
Pam2Cys9	Pam2	CGNDDGKDKDG	+++
Pam2Cys10	Pam2	CGNNSSKDKEA	+++
Pam2Cys11	Pam2	CSLPGLGSKST	+++
Pam2Cys12	Pam2	CSTSEVIGEKI	++
Pam2Cys13	Pam2	CPFNCVGCYNK	+/−
Pam2Cys14	Pam2	CGSQNLAPLEEK	+/−
Pam2Cys15	Pam2	CLILIIASETL	+/−
Pam2Cys16	Pam2	CLILIIASETLFSFSHLTDVK	+/−
Pam2Cys17	Pam2	CSK	n.d.
Pam2Cys18	Pam2	CSKK	n.d.
Pam2Cys19	Pam2	CSKKKK	++

*100 pg/ml of Pam2 peptides were used for stimulation of PBMC.
TNF-α levels: +/−; <200, ++; 2,000–4,000, +++; 4,000–7,000 pg/ml.
n.d., not determined.
doi:10.1371/journal.pone.0012550.t001

The degree of CD86 upregulation by the 16 *S. aureus* lipopeptides was examined, and similar DC maturation profiles were obtained by flow cytometer for all Pam2Cys tested (Fig. 1D), suggesting BMDC maturation, as determined by CD86 up-regulation, was independent of NF-kB activation or cytokine liberation by these lipopeptides.

NK activation by Pam2Cys peptides

Previous reports suggested that TLR2 agonists can induce NK activation [22–24]. To investigate whether the *S. aureus* lipoproteins had NK cell-activating activity, we added the Pam2Cys peptides at 100 nM to BMDC/NK cultures as described previously [4]. Three markers for NK activation [26] were assessed: IFN-γ production, up-regulation of NK surface markers, and target B16D8 cell cytotoxicity by NK cells (Fig. 2). IFN-γ was generated in the supernatants (sup) in response to the lipopeptides (Fig. 2A). However, Pam2Cys13, Pam2Cys15, and Pam2Cys16 showed significantly low potential for IFN-γ induction as comparable to Pam2Cys17. Cytotoxic activity was evaluated using B16D8 cells as a target [4]. Again, Pam2Cys13, 15 and 16 did not induce effective killing (Fig. 2B). The other *S. aureus* lipopeptides had sufficient killing activity: two simultaneously generated examples are shown in Figure 2B.

The NK cell activation markers CD25 and CD69 were analyzed by flow cytometry after co-culturing NK cells with BMDC and Pam2Cys stimulants (Fig. 2C). Up-regulation of

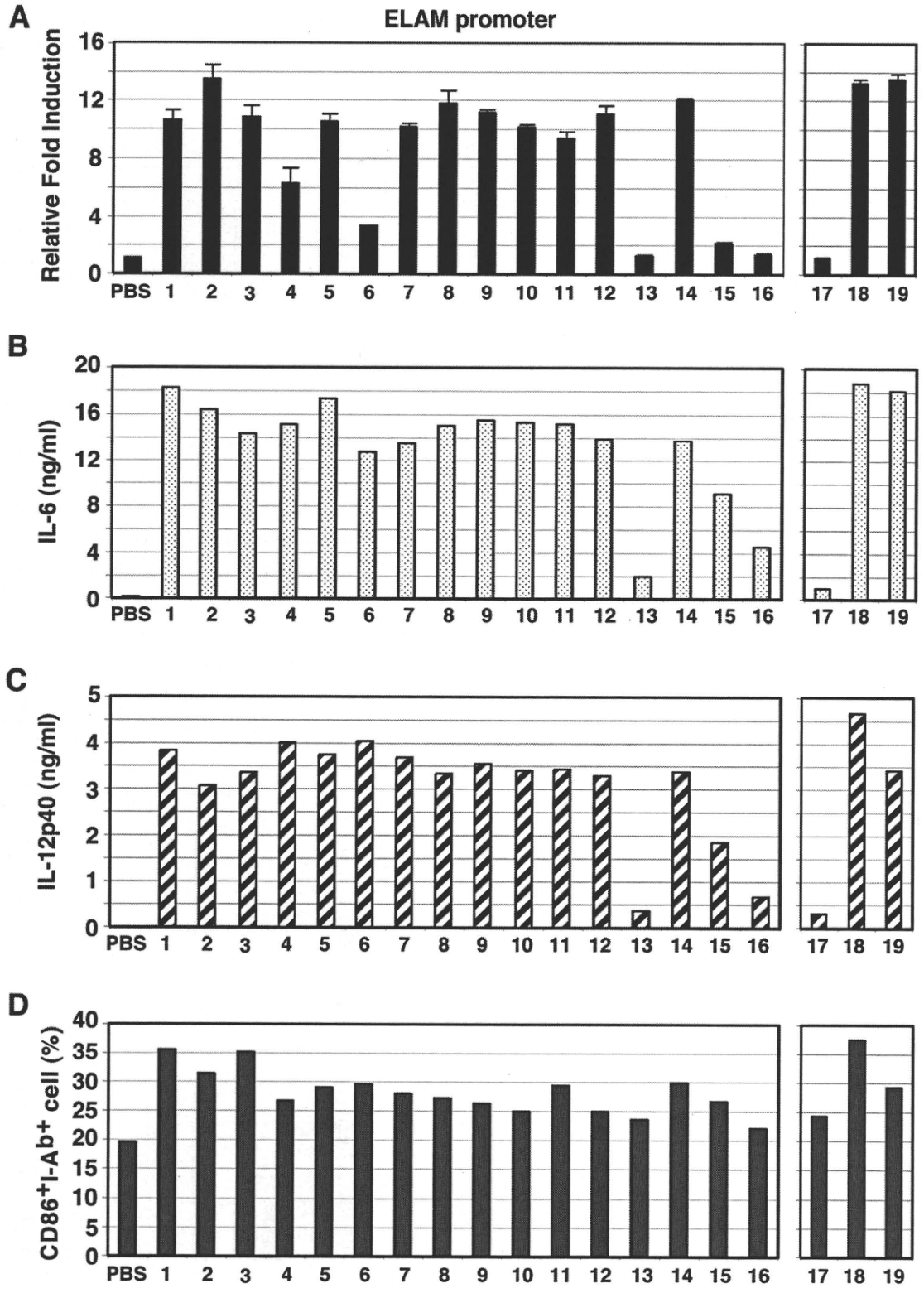

Figure 1. Synthetic Pam2Cys lipopeptides activate TLR2 and induce cytokine production in BMDC. (A) HEK293 cells were transfected with plasmids encoding TLR2 and ELAM-luciferase reporter. After 24 h, the cells were treated with Pam2Cys peptides (100 nM) for 6 h and then luciferase activities of the cell lysates were measured. (B, C) BMDC were treated with Pam2Cys peptides for 24 h and IL-6 and IL-12p40 concentrations in the culture supernatants were measured by ELISA. (D) CD86 and MHC class II (I-Ab) expression of the BMDC were determined by flow cytometry. Data represents the mean ± SD of triplicate measurements. The data shown are representative of at least three independent experiments. The numbers represent the Pam2Cys's numbers.
doi:10.1371/journal.pone.0012550.g001

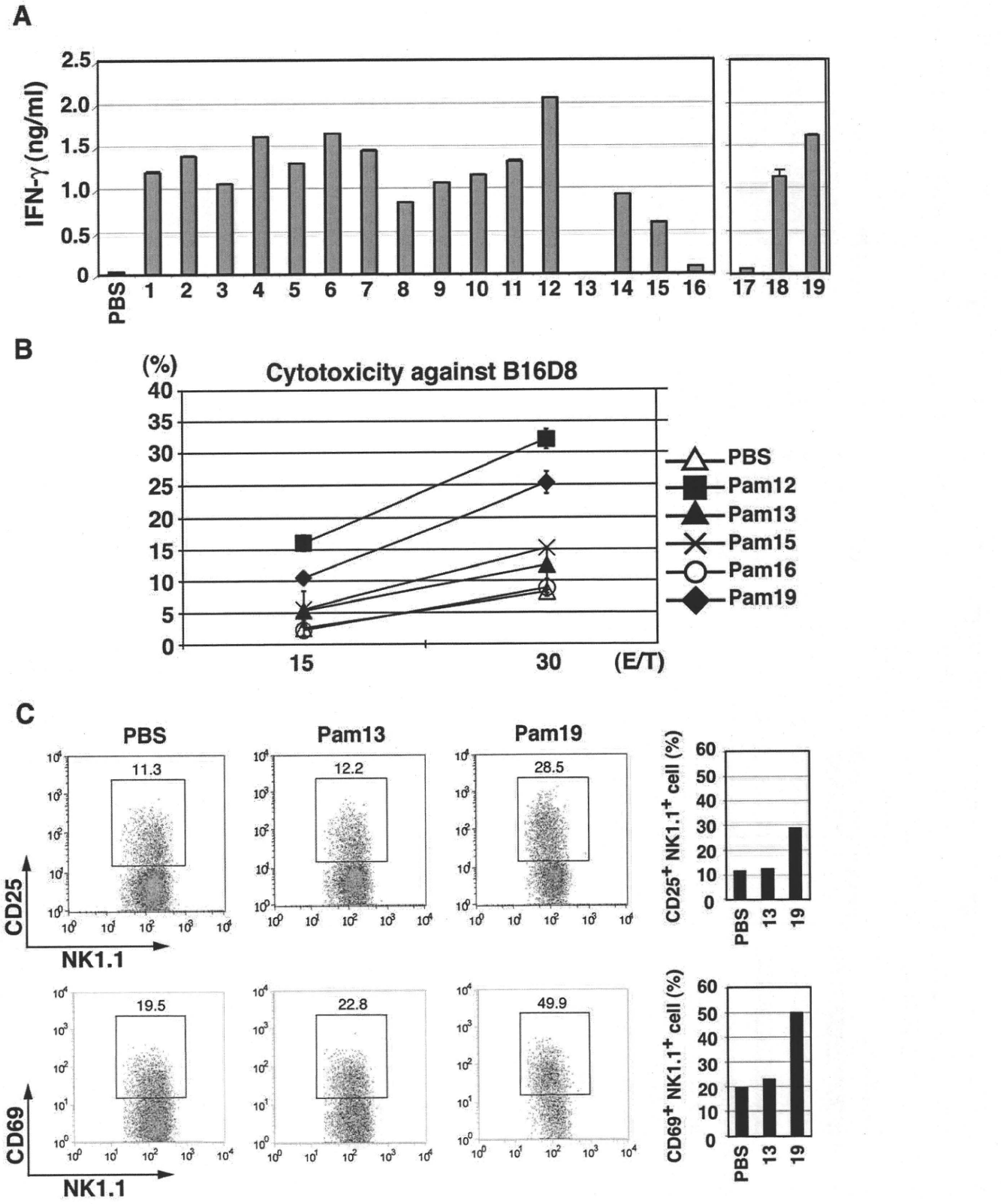

Figure 2. Pam2Cys peptides activate NK cells via BMDC. (A) Wild-type BMDC and wild-type NK cells were co-cultured at 1:2 ratio in the presence of Pam2Cys peptides as the numbers indicated (100 nM). After 24 h, IFN-γ concentrations in the supernatants were measured by ELISA. (B) NK cell cytotoxicity against B16D8 cells was measured by ^{51}Cr release assay at indicated E:T ratios as described in the Methods section. (C) Populations of CD25+ and CD69+ NK cells were measured by flow cytometry after stimulation of NK cells with BMDC treated with indicated Pam2Cys peptides. BMDC were stimulated with control PBS, 100 nM of Pam2Cys13 or Pam2Cys19 for 4 h. Then, BMDC were incubated with NK cells. After 24 h, cells were analyzed by flow cytometer using the markers for separation. %Positive cells are shown to the right.
doi:10.1371/journal.pone.0012550.g002

surface CD25 and CD69 was observed in NK cells incubated with BMDC and Pam2Cys18 or 19, while the levels of their up-regulation by Pam2Cys13, 15 or 16 were near those of the negative control Pam2Cys17, for stimulating NK cells co-cultured with BMDC. In contrast, no increase was observed for CD56, NKp46 and DNAM-1 (data not shown).

Participation of TLR2/MyD88 in Pam2Cys-mediated BMDC and NK activation

Activated NK cells are a major source of IFN-γ, which causes a variety of responses in the immune system. To examine whether direct stimulation of NK cells with Pam2Cys18 or Pam2Cys19 induced secretion of IFN-γ, we measured the frequency of IFN-γ-secreting NK cells, at 24 h after incubation. By intracellular staining, IFN-γ-secreting NK cells were increased after direct Pam2Cys18 or 19 stimulation (data not shown). As shown in Figure 3A and B, TLR2 ligands except Pam2Cys12, 18 and 19 barely increased the levels of IFN-γ of NK cells by co-culture with Pam2Cys-stimulated TLR2−/− or MyD88−/− BMDC. On the other hand, NK cells induce moderate levels of IFN-γ in response to BMDC stimulated with Pam2Cys12, 18 or 19 (open bars in Figure 3A), although no structural similarity was detected between Pam2Cys12 and Pam2Cys18 or 19.

We next examined whether lipopeptide-mediated cytokine secretion and NK activation were dependent on BMDC TLR2 and MyD88. IL-6 and IL-12p40 secretion were completely abrogated in TLR2−/− BMDC (data not shown). However, low amounts of IFN-γ were detected in co-cultures of TLR2−/− or MyD88−/− BMDC and wild-type (WT) NK cells in the presence of Pam2Cys12, 18, or 19 (Fig. 3B,D), and lesser extent of IFN-γ was still detected in co-cultures of WT BMDC and TLR2−/− NK cells in the presence of Pam2Cys12 or Pam2Cys19 (Fig. 3C). These results were reproduced with MyD88−/− BMDC (not shown). Notable results are shown in Fig. 3D where WT or TLR2−/− BMDC were stimulated with indicated Pam2Cys and incubated with WT or TLR2−/− NK cells. Moderate IFN-γ was detected in the media containing TLR2−/− BMDC, WT NK and Pam2Cys12 or 19 (Fig. 3D), the IFN-γ levels being comparable to those of WT NK cells alone stimulated with Pam2Cys12 or 19 (Fig. S1). TLR2−/− NK cells still produced very low levels of IFN-γ when the TLR2−/− NK cells were co-cultured with WT BMDC (Fig. 3D). However, No IFN-γ was detected in the media containing TLR2−/− NK and Pam2Cys12 or 19. Thus, all Pam2Cys peptides including Pam2Cys12, 18 and 19 act on BMDC to drive NK activation. Notably, WT NK cells alone produce minute IFN-γ in response to Pam2Cys12 or 19 (Fig. S1), which means that Pam2Cys12 and Pam2Cys19 additionally induce direct NK activation. The Pam2Cys receptors for this NK activation is through the NK cell TLR2 followed by the MyD88 pathway. However, minute activation by Pam2Cys12 or 18/19 appears to be left in TLR2−/− NK cells stimulated with Pam2Cys12/19-treated BMDC, which should be attributed not to TLR2 but to other unknown mechanisms.

Combinatorial recognition of Pam2Cys lipopeptide by TLR2 and TLR6

TLR2 recognizes diacyl lipopeptides in combination with TLR6 [14,31] while TLR2 recognizes triacyl lipopeptide with TLR1 [15,32]. We found TLR2/6 cooperation in the recognition of *S. aureus* lipopeptides using HEK293 cells that express TLR2/6. Data on the use of TLR2/6 by Pam2Cys12, Pam2Cys13, Pam2Cys15, Pam2Cys16, and Pam2Cys19 is shown in Figure 4. Single receptors of TLR1, TLR6, and TLR10 showed little activation of NF-κB by reporter assay, and only TLR2 exhibited <60-fold ELAM promoter activation (data not shown). Pam2Cys12 and Pam2Cys17 more efficiently activated the ELAM promoter (>300 fold over the control) with TLR2 and 6, than with TLR2 alone (Fig. 4A). TLR1 or TLR10 in combination with TLR2 did not amplify the signal (Fig. 4B). Pam2Cys13 only weakly enhanced the TLR2 potential with additional TLR6 expression in HEK cells (Fig. 4A), and only a slight increase was observed with Pam2Cys15 and Pam2Cys16 with simultaneous expression of TLR2 and TLR6 (Fig. 4A). Hence, TLR6 helped TLR2 to amplify the TLR2 signal from most Pam2Cys lipopeptides, but not with Pam2Cys13 or Pam2Cys15/16.

Critical a.a. in Pam2Cys lipopeptides for BMDC-mediated NK activation

Recent studies revealed an extensive cross-talk between NK cells and mDCs [2,6]. We analyzed the structural background that supports NK activation using our synthetic diacyl lipopeptides. All NK-activating lipopeptides tested had Cys-Ser/Thr or Cys-Gly/Ala in their N-terminus (Table 1). However, the two lipopeptides with the lowest ability to activate NK cells had differences, with Cys-Pro in the N-terminus of Pam2Cys13, and Cys-Leu-Ile in Pam2Cys15/16. When the second Pro in Pam2Cys13 was replaced with Ser, and the Leu-Ile sequence of Pam2Cys16 was replaced with Ser-Asn, the newly synthesized peptides, Pam2-Cys13(P-S) and Pam2Cys16(LI-SN), recovered their ELAM reporter activity (Fig. 5A).

We next tested whether BMDC mature to activate NK cells through BMDC's TLR2 activation by these modified Pam2Cys. Pam2Cys13(P-S) and Pam2Cys15(LI-SN) recovered NK-activating properties by the amino acid conversions judged by IFN-γ production (Fig. 5B) and cytotoxicity against B16D8 cells (Fig. 5C). Since Pam2Cys13(P-S) acts only on BMDC (not shown), this Pam2Cys activity is attributable to recovered BMDC maturation. Hence, Pam2Cys13(P-S) and Pam2Cys16(LI-SN) are NK activators via mDC TLR2. Hence, we conclude that the peptide sequence near the N-terminus is important for NK activation by diacyl lipopeptide.

Production of both IL-6 and IL-12p40 was dependent on BMDC TLR2 (Fig. 6A). Pam2Cys13 and Pam2Cys16 induced these cytokines at very low levels. When Pam2Cys13(P-S) or Pam2Cys16(LI-SN) replaced Pam2Cys13 or Pam2Cys16 in the same assay system, the cytokine levels recovered to levels similar to those of the other lipopeptides (Fig. 6B). These activities were almost completely abrogated in TLR2−/− BMDCs. Thus, the a.a. replacements allows BMDC to generate the TLR2 signal, irrespective of their artificial modifications.

BMDC-NK contact is indispensable for BMDC TLR2-mediated NK activation

Pam2Cys13(P-S) matured BMDC to activate NK cells without direct action on NK cells (Fig. 7A). First, we collected the sup of BMDC stimulated with Pam2Cys13 or Pam2Cys13(P-S). Surprisingly, Both of the sup failed to confer NK activating function on the mixture of naïve BMDC and NK cells (data not shown). The capacity of BMDC sup to induce IFN-γ-secretion by NK cells was further evaluated using a transwell system (Fig. 7A,B). No significant increase in IFN-γ-secreting NK cells was observed when lipopeptide-activated BMDCs and NK cells were separated by transwell (Fig. 7A,B). Frequency of IFN-γ-producing NK cells was high in co-culture with Pam2Cys13(P-S)-stimulated BMDC and NK cells (Fig. 7B upper panel) while the IFN-γ-producing NK

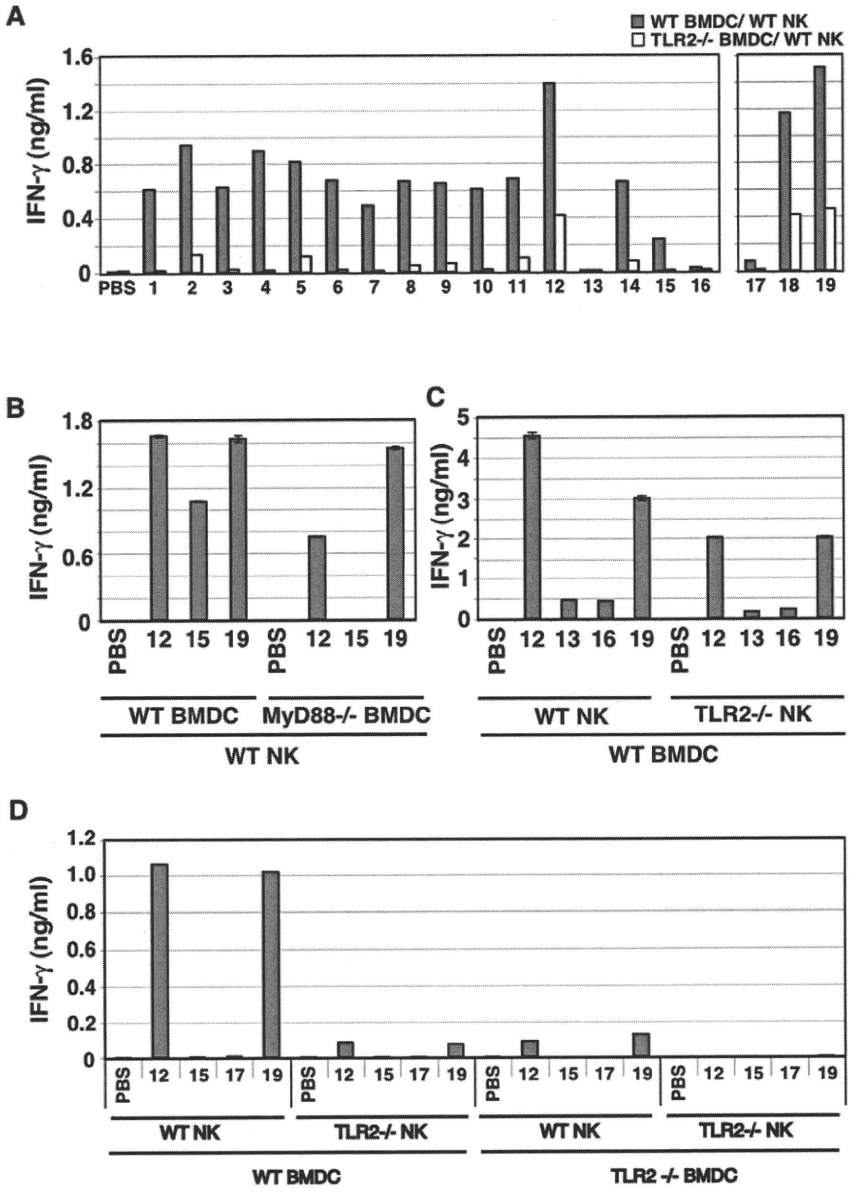

Figure 3. TLR2 on BMDC mainly participate in Pam2Cys-mediated NK activation. (A) BMDC TLR2-independent NK activation by Pam2Cys12, 18 and 19. BMDC from wild-type (closed bars) or TLR2−/− (open bars) mice were stimulated with control PBS or 100 nM of indicated Pam2Cys peptides for 4 h. Cells were then co-cultured with wild-type NK cells at 1:2 ratio for 24 h. Then, the supernatants were collected and IFN-γ was measured by ELISA. (B) Pam2Cys12 and 19 induce NK activation in culture with MyD88−/− BMDC. NK cells were co-cultured with wild-type or MyD88−/− BMDC in the presence of the indicated Pam2Cys peptides (represented by the numbers) as in Fig. 2. 24 h after incubation, culture media were collected to determine cytokines by ELISA. (C) Pam2Cys12 and 19 induce TLR2−/− NK activation in culture with wild-type BMDC. Wild-type BMDC and NK cells with either wild-type or TLR2−/− phenotype were incubated at 1:2 ratio with the indicated Pam2Cys peptides (represented by the numbers) as in Fig. 2. 24 h after incubation, culture media were collected to determine cytokines by ELISA. One representative of the three similar experiments is shown. (D) TLR2 NK cells mainly participates in TLR2 BMDC-independent NK activation by Pam2Cys12 and 19. Wild-type and TLR2−/− BMDC were stimulated with indicated Pam2Cys peptides for 4 h. These BMDC were then mixed with NK cells as shown in the panel. Four groups consisting of either of wild-type NK or TLR2−/− NK and either of wild-type BMDC or TLR2−/− BMDC (see the bottom of the panel) were incubated with the indicated Pam2Cys peptides (50 nM) for 24 h. NK cells alone with Pam2Cys12 or 19 liberated minure IFN-γ as in the panel with WT NK + TLR2−/− BMDC (see Fig. S1). IFN-γ concentrations in the culture supernatants were determined by ELISA. The data shown are representative of at least three independent experiments.
doi:10.1371/journal.pone.0012550.g003

cells were diminished in the transwell (Fig. 7B lower panel). In either case, IL-15 and IFN-α/β were barely increased in Pam2Cys-stimulated BMDCs by RT-PCR (data not shown). Thus, soluble factors barely participate in BMDC-mediated NK activation. BMDC-NK contact is essential for TLR2-mediated NK activation.

Discussion

Here, we demonstrated that the a. a. sequence of *S. aureus* Pam2Cys peptides critically affects the agonistic function for TLR2 and the mode of NK activation. This NK activation is largely dependent on TLR2/MyD88 in BMDC in the mouse

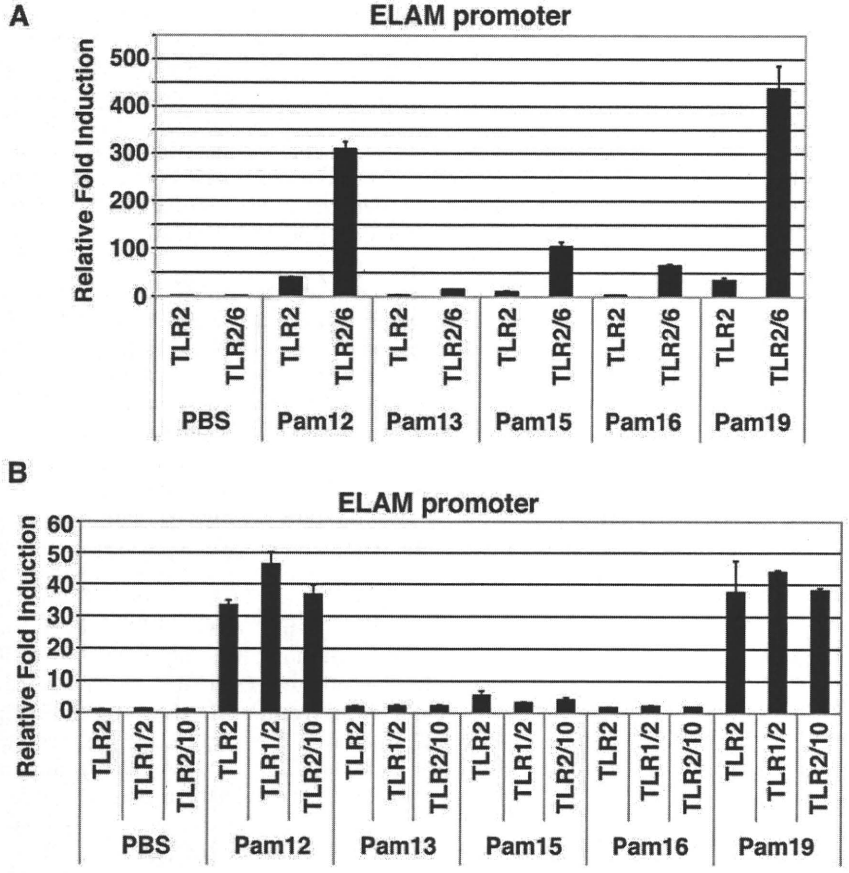

Figure 4. TLR6 promotes TLR2 signaling in Pam2Cys peptides recognition. (A, B) HEK293 cells were transfected with plasmids encoding TLR2, TLR6, TLR1 or TLR10 and the ELAM-luciferase reporter. After 24 h, the cells were treated with indicated Pam2Cys peptides (100 nM) for 6 h and then luciferase activities were measured. The data shown are representative of at least three independent experiments.
doi:10.1371/journal.pone.0012550.g004

system. In addition, Pam2Cys12 and Pam2Cys18/19 have a weak ability to directly activate NK cells without participation of BMDC. In contrast, we determined Pam2Cys13, Pam2Cys15, and Pam2Cys16 to be dysfunctional, since these lipopeptides failed to activate TLR2/6 reporter signaling or induce cytokines in BMDC (Fig. 1,4). Although the first Cys is conserved in all the lipopeptides tested, the following sequences varied, even though all showed BMDC maturation activity. Notably, the second a. a. residue was Ser/Thr or Gly/Ala in the functional lipopeptides, followed by undefined sequences. A length of more than three a.a. was indispensable for BMDC-mediated NK activation (Fig. 1, Pam2Cys17 vs. 18). The failure of Pam2Cys13, Pam2Cys15, and Pam2Cys16 to activate NK cells suggests the importance of the second and/or third residue for stimulating BMDC or directing NK activation. Pam2Cys13 harbors Pro in the second residue, which breaks hydrogen bond interactions. Likewise, Pam2Cys15 and Pam2Cys16 commonly possess Leu and ILe in the second and third residues, which also destabilize hydrogen bond interactions. Thus, these a. a. residues critically influence the effectual interaction between the Pam2Cys peptides and the TLR2 complex on either BMDC or NK cells.

TLR2 initiates immune response by recognizing diacylated lipoproteins in combination with TLR6. We surmise that this receptor complex recognizes the a. a. properties in the peptide sequence that activate mDC/NK cells. Crystal structure analysis indicates that hydrogen bonds between glycerol and the peptide backbone of the ligand and the leucine-rich repeat (LRR)11 loops of TLRs are critical for TLR heterodimerization [31,32]. These hydrogen bonds bridge TLR2 and TLR6 with the ligand, and fix the conformation of the hydrophobic residues around the dimerization interface [31]. The side chains of the first two a. a. of Pam2Cys have substantial interactions with the TLRs. The N-terminal Cys binds to the sulfur site formed by the hydrophobic F325, L328, F349, L350, and P352 residues of TLR2, and the L318 residue of TLR6 [31]. The hydroxyl side chains of the second Ser/Thr form a medium-range hydrogen bond with the F325 backbone of TLR2. As seen in the TLR2/TLR6/Pam2CSK4 structure, the side chains beyond the third lysine residue have highly flexible structures and form only weak ionic or hydrogen bond interactions with the TLRs [31]. Hence, our results with a. a. substitutions fit the proposed TLR2-Pam2CSK4 interacting model.

In a previous report, lysines in the triacyl peptide were seen to form hydrogen bonds with TLRs when Pam3CSK4 interacts with TLR2/TLR1 heterodimer [32]. The ε-amino residues in the side chains appear to participate in lipopeptide recognition by TLRs [31,32]. In our results, the small side chains of Asn or Gly had no blocking effects on the peptide-TLR2 interaction (data not shown). Thus, a hydrophilic or small a. a. in the chain barely altered the lipopeptide function exerted through TLR2. The *S. aureus* lipopeptides, with the exception of Pam2Cys13, Pam2Cys15, and Pam2Cys16 are compatible with this principle. We actually demonstrated here that the peptide sequences have a significant effect on the immunological activity of the lipopeptides. The recognition system for bacterial lipoproteins has developed to

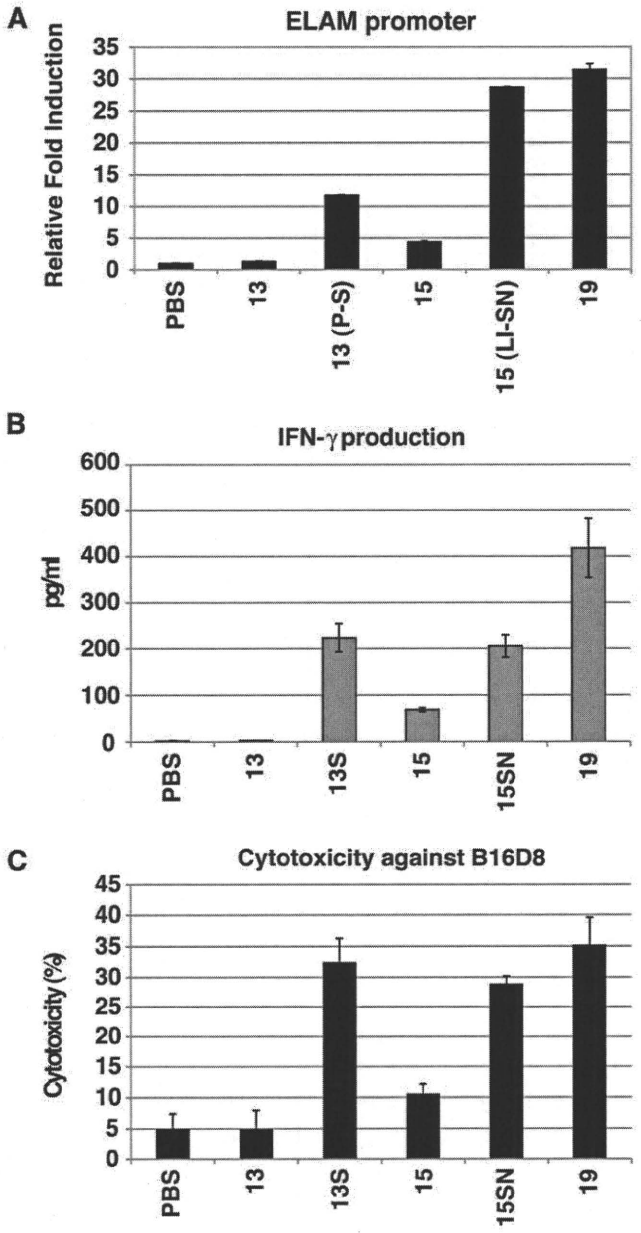

Figure 5. Amino acids near the Pam2 lipid are critical for TLR2 recognition. (A) HEK293 cells were transfected with plasmids encoding TLR2 and the ELAM-luciferase reporter. After 24 h, the cells were treated with indicated Pam2Cys peptides (100 nM) for 8 h and then luciferase activities were measured. The numbers represent the Pam2Cys's numbers. 13(P-S), Pam2Cys13 with second Proline replaced with Serine; 15(LI-SN), Pam2Cys15 with second Leucine and third Isoleucine replaced with Serine and Asparagine. (B,C) BMDC-mediated NK cell activation occurs by stimulation with Pam2Cys13 (P-S) and Pam2Cys15 (LI-SN). BMDC and NK cells were prepared from wild-type mice. BMDC were stimulated with PBS or indicated Pam2Cys peptides for 4 h. Then, BMDC were incubated with wild-type NK cells for 24 h. IFN-γ production (A) and B16D8 cytotoxicity (E:T ratio = 50:1) (B) were measured as in Figure 2. 13S and 15SN represent Pam2Cys13(P-S) and Pam2Cys15(LI-SN), respectively.
doi:10.1371/journal.pone.0012550.g005

sense common structures of the lipid, as well as the peptide sequences.

The factor that determines whether mDC TLR2 or NK TLR2 predominates in diacyl lipopeptide activation has remained to be settled. The sequence information about the NK-activating vs. DC-activating lipopeptides in this study suggests that lysines or hydrophilic a. a distal to Pam2Cys are involved in this selective activity. Peptides with lysines tended to exert direct NK activation. According to the structural studies [31,32], the lysines in Pam3CSK4 form multiple hydrogen bonds with TLR2/1, and the same is expected to be true of Pam2CSK4 and TLR2/6. Hence, hydrophilic residues after the second residue of the Pam2Cys lipopeptides may participate in high affinity interaction with NK cell TLR2/6.

In a previous report, we identified the NK-activating protein INAM, which discrminates between active and resting NK cells, and reflects *in vivo* tumoricidal action of NK cells [33]. INAM is expressed on polyI:C-matured mDCs in response to IRF-3 activation, and is not expressed on mDCs stimulated with TLR2 agonists [33]. In both TLR2- and TLR3-stimulation, IFN-γ is a marker of NK activation [4,6,22,33], almost parallel to NK cell-mediated target cytotoxicity. According to these criteria, mDC drive NK activation via two arrays, MyD88 and TICAM-1 pathways. Anyhow, the MyD88-mediated NK activation occurs independently of TICAM-1-mediated NK activation. Here we provide further knowledge on the MyD88-mediated NK activation: mDC TLR2-dependent, and mDC TLR2-independent pathways exist for NK activation. The latter involves NK TLR2-dependent NK activation, where the lipopeptides directly stimulate TLR2 and the MyD88 pathway in NK cells. However, a minimal NK-activating capacity by Pam2Cys12, 18 and 19 retains in TLR2−/− NK cells. This means that the direct NK activation largely depends on NK cell TLR2/MyD88 but does not neglect participation of other undetermined factors, such as NOD-like receptor (NLR) family, either in mDC or NK cells.

Pam2Cys-matured BMDC produce IL-12 by the MyD88 pathway. Unexpectedly, however, results from transwell studies did not support the importance of IL-12 in NK activation. In addition, NK-activating cytokines, such as IL-15 and IFN-α/β, are barely increased in Pam2Cys-stimulated BMDC (data not shown). Cell-cell contact rather than soluble mediators is crucial for mDC TLR2-mediated NK activation in this study.

Taken together, we showed that *S. aureus* lipopeptides induce mDC-mediated NK activation. It is intriguing that this is a case of the reported reciprocal activation [2], in which ligands-receptors on mDC and NK cells are involved. In a. a. sequences of Pam2Cys, lysine distal to the N-terminal Pam2 and hydroxyl residues proximal to the Pam2 affect NK-activating potential through its interaction with TLR2. When bacteria invade host tissue, they encounter many proteases. Since plasma serine proteases frequently cleave the Lys-X sequence of substrates, the lipoproteins may be clipped out into liberated lipopeptides containing Lys, which could be important in the context of TLR2-induced inflammatory immune responses. In fact, after completing this manuscript, two in press papers were released where some bacterial components are shown to participate in TLR2-mediated NK activation [34,35]. Our findings furthered these notions by analyzing synthetic Pam2Cys peptides under the knowledge of the structural background of TLR2 [31,32].

A question remaining is why bacteria provide two sorts of lipopeptides with TLR2-activating and –nonactivating properties. So far, we have no experimental finding to sufficiently answer this question, but bacterial infection usually alters host inflammatory milieu and recruits immune competent cells to the lesion [36]. In this context, it is not surprising that Pam2Cys lipopeptides serve as modifiers for host immune response against bacteria. Different responses could be expected to occur with various combinations of Pam2Cys peptides in infectious lesion. Here we demonstrate that

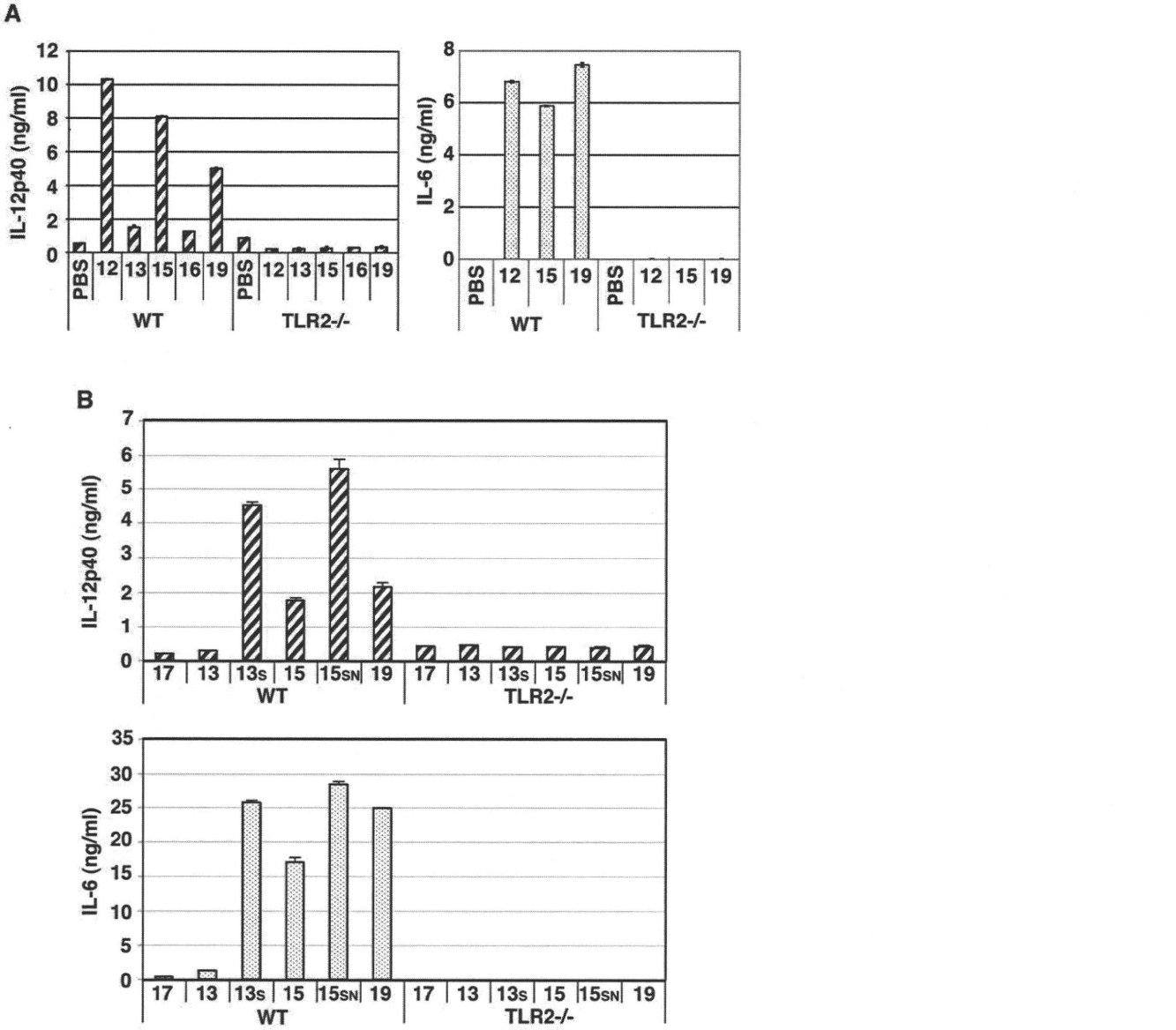

Figure 6. TLR2 agonists in BMDC is crucial for IL-6 and IL-12 production. (A) IL-6 and IL-12p40 production by wild-type but not TLR2−/− BMDC by Pam2Cys stimulation. BMDC prepared from wild-type or TLR2−/− mice were treated with indicated Pam2Cys peptides (100 nM) for 24 h. IL-12p40 and IL-6 concentrations in the supernatants were determined by ELISA. (B) Pam2Cys13(P-S) but not Pam2Cys13 induces IL-6 and IL-12 from BMDC. BMDC prepared from wild-type mice were treated with indicated Pam2Cys peptides (100 nM) for 24 h as in panel A. Cytokines in the supernatants were determined by ELISA. 13S, Pam2Cys13(P-S); 15SN, Pam2Cys15(LI-SN).
doi:10.1371/journal.pone.0012550.g006

NK activation is a phenotype induced by TLR2-activating bacterial lipopeptides, which properties are determined by the peptide sequence of the Pam2Cys. Studies on these functional behaviors of lipopeptide towards mDC and on how TLR signals link NK activation in bacterial infectious diseases will be the next highlight for understanding the importance of early phase of innate cellular response against various bacterial infections.

Materials and Methods

Reagents and antibodies

The following materials were obtained as indicated: Fetal calf serum (FCS) from Bio Whittaker (Walkersville, MD), mouse granulocyte-macrophage colony-stimulating factor (GM-CSF) from PeproTech EC, Ltd (London, UK), polymyxin B from SIGMA-Aldrich (St. Louis, MO), Pam2CSK4 was in part purchased from Amersham Pharmacia Biotech (Piscataway, NJ) and Lympholyte-M from Cedarlane (Ontario, Canada). The enzyme-linked immunosorbent assay (ELISA) kits for mouse (m)IFN-γ from eBioscience (San Diego, CA), and IL-12p40 and IL-6 from Amersham Biosciences.

The following antibodies were used: mAbs against mouse CD11c, NK1.1, CD86, I-Ab, CD25, CD69, DNAM1, CD56 and NKp46 were purchased from BioLegend (San Diego, CA).

Preparation of synthetic peptides

The synthesis of lipopeptides was achieved with a combination of solution- and solid-phase methods [30]. Briefly, for the preparation of the Pam2Cys backbone, the protected cysteine (Fmoc-Cys-OtBu) and the iodide (3-iodopropane-1,2-diol) were

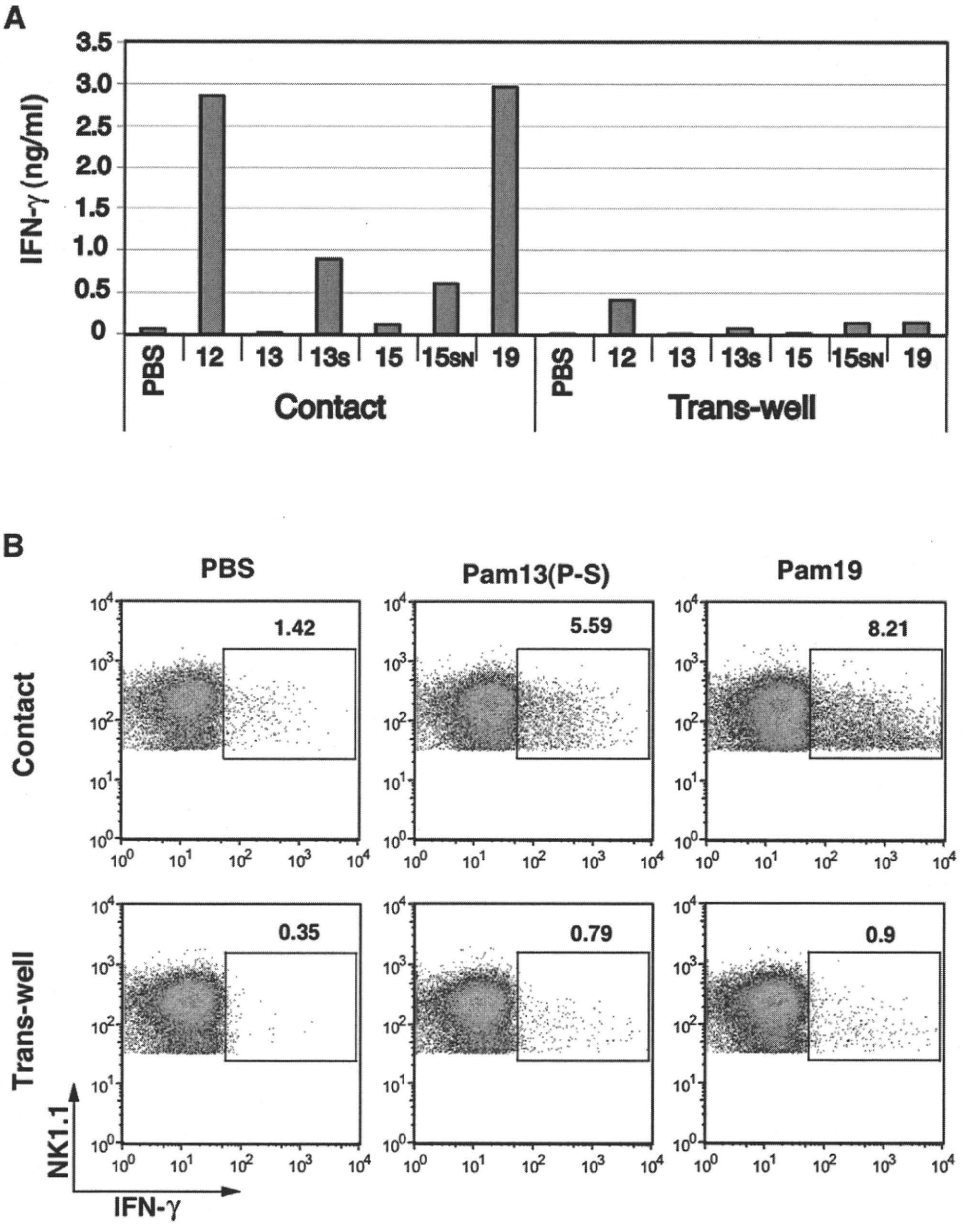

Figure 7. BMDC-NK cell contact induces NK activation. (A) IFN-γ induction by NK cells requires BMDC-NK contact. BMDC prepared from wild-type mice were treated with indicated Pam2Cys peptides (100 nM) for 4 h. Then, BMDC were incubated with naïve NK cells for 24 h at the ratio of 1:2 (left hand bars in Contact). The level of IFN-γ was measured by ELISA. Of note, the sup of the stimulated BMDC was collected and added to cultures of unstimulated BMDC and naïve NK cells, but only a minute level of IFN-γ was detected in the sup (data not shown). The levels of IFN-γ in the same combinations are shown (right hand bars in Trans-well) when stimulated BMDC and NK cells were separated by trans-well. 13S, Pam2Cys13(P-S); 15SN, Pam2Cys15(LI-SN). (B) %IFN-γ-positive NK cells were determined by intracellular staining. Wild-type BMDC prepared from C57BL/6 mice were treated with Pam2Cys13(P-S) peptides (100 nM) for 4 h as in panel A. Then, wild-type NK cells were added to the wells. 20 h after co-culture, breferdin was added to the wells and incubation was continued further for 4 h. NK cell activation was determined by IFN-γ produced in NK cells. %IFN-γ-positive NK cells was determined by FACS.
doi:10.1371/journal.pone.0012550.g007

coupled under basic condition by using Cs_2CO_3 to give Fmoc-Cys(2,3-dihydroxypropyl)-OtBu, and the subsequent acylation and cleavage of the tBu group gave Fmoc-Pam2Cys-OH [37]. The peptide component, which included 16 different peptide sequences from 14 lipoproteins of *S. aureus* NCTC8325, was prepared by using solid-phase synthesis on Wang resin in a similar fashion to Jung's lipopeptide synthesis. Fmoc-Pam2Cys-OH [30,37] was then introduced to the N terminus of the peptides linked to the resin. Subsequent cleavage of the Fmoc group, detachment from the resin, and deprotection of all protecting groups gave the lipopeptides Pam2Cys1–16, and also Pam2CSK4. Pam2CSK and Pam2CSK2 were obtained from Biologica Co. Ltd. Commercial and our synthetic Pam2CSK4 had indistinguishable potential for BMDC maturation and cytokine production (data not shown).

Mouse and cell lines

TLR2 −/−, TLR4 −/−, and MyD88 −/− mice were gifts from Dr. S. Akira (Osaka Univ., Osaka) as previously reported [9].

TICAM-1 (TRIF) −/− and IPS-1 −/− mice were established in our laboratory [4,33]. Female C57BL/6 mice were purchased from Clea Japan (Tokyo). Mice were maintained in our institute under specific pathogen-free conditions. All animal work was performed under guidelines established by the Hokkaido University Animal Care and Use Committee. This study was approved as Analysis of immune modulation by toll-like receptors by this committee. Mice (12 weeks female C57BL/6) were housed four per cage and allowed food and water ad libitum. The Ethics committee in Hokkaido University approved this study (ID number: 08-0243). Animal studies were carefully performed without ethical problems.

B16D8 were established in our laboratory as a subline of the B16 melanoma cell line [38]. This subline was characterized by its low MHC levels with no metastatic properties when injected s.c. into syngeneic C57BL/6 mice [4,33]. HEK293 and B16D8 cell lines were obtained from ATCC (USA). These cell lines were cultured in RPMI 1640/10% FCS.

Preparation of BMDCs and spleen NK cells of mice

Mouse bone marrow-derived DC (BMDC) were prepared as described previously [4]. Spleen NK cells were positively isolated from spleens with DX5 Micro Beads (Miltenyi Biotech) [33]. In experiments requiring high purity NK cells, Thy1.2 beads were additionally used for negative selection according to the Miltenyi's protocol. The purity of NK cells ($DX5^+$ cells) was routinely about 70%. NKT cells might be an only trace constitution of our preparation. $DX5^+$ NK cells were used within 24 h.

Reporter assay

Plasmids (pEFBos) for expression of human TLR1, TLR2, TLR6 and TLR10 were prepared in our laboratory as described previously [39]. HEK293 cells were seeded onto 24-well plates and transfected with 0.1 μg TLR expression vectors, 0.1 μg of ELAM-1, and 0.05 μg of phRL-TK control plasmid using FuGene HD (Roche) according to the manufacturer's instructions. The ELAM-luciferase reporter plasmid was made in our laboratory [13]. After 24 h, the cells were harvested in 50 μl lysis buffer. The luciferase activity was measured using Dual-Luciferase Reporter assay systems (Promega) and was shown as the means ± S.D. of at least three experiments.

Statistical analysis

Student's *t* test was used to examine the significance of the data when applicable in quantitative studies. Differences were considered to be statistically significant when $P<0.05$.

ELISA, Flow cytometric (FACS) analysis of cell surface antigens

The levels of cytokines (IL-6, IL-12p40, IFN-γ etc.) were determined by sandwich ELISA (Amersham Pharmacia Biotech, Buckinghamshire, UK) or the message levels assessed by quantitative PCR [38]. Surface CD25, CD86 and CD69 levels were determined by FACS using specific mAbs. The practical methods for FACS were described previously [40]. Intracellular staining of IFN-γ was peformed with breferdin-treated NK cells as described previously [39]. Trans-well analysis was performed as described previously [40]. Assays were usually performed at least three times in duplicate, otherwise indicated in the legends, and one representative experiment is shown.

Assessment of in vitro cytolytic activity

The cytolytic activity of spleen NK cells was determined by ^{51}Cr assay as described previously [4,33]. NK cells were prepared from the spleen of intact C57BL/6 mice. NK cells were co-cultured with BMDCs at a ratio of 2:1 and 24 h later the mixtures were subdivided to assess NK-mediated cytotoxicity [4]. A B16 subline (D8) or YAC-1 was used as a target cell. Target cells (2×10^3 cells/well) were coincubated with NK cells at the indicated lymphocyte to target (E/T) cell ratio (typically 5, 15 and 30) in U-bottom 96-well plates in a total volume of 200 μl of 0.5% BSA/RPMI-1640 medium at 37°C. Four hours later, the liberated ^{51}Cr in the medium was measured using the scintillation counter. Specific cytotoxic activity was obtained by the formula: Specific cytotoxic activity (%) = [(experimental ^{51}Cr activity - spontaneous ^{51}Cr activity)/(total ^{51}Cr activity − spontaneous ^{51}Cr activity)] ×100. Each experiment was done in triplicate to confirm reproducibility of the results, and representative results are shown. *t* test was used to examine the significance of the data.

Supporting Information

Figure S1 Direct activation of NK cells by stimulation with Pam2Cys12, 18 or 19. Wild-type or TLR2−/− NK cells (5×105 cells/well) were stimulated with indicated Pam2Cys peptides for 24 h. After 24 h, IFN-γ concentrations in the supernatants were measured by ELISA as in Fig. 2A. The IFN-γ concentrations were more than 5-fold lower than those in the mixture of BMDC and NK cells (see Figs. 2A and 3).
Found at: doi:10.1371/journal.pone.0012550.s001 (0.08 MB TIF)

Acknowledgments

We thank Drs. M. Sasai, J. Kasamatsu, H. Takaki, H. Shime, A. H. Hussein, A. Watanabe and H. Oshiumi in our laboratory for their critical discussions. Thanks are also due to Mr. Negishi for his technical assistance. Gifts of TLR2−/− and MyD88−/− mice from Drs. S. Akira are gratefully acknowledged.

Author Contributions

Conceived and designed the experiments: YA TE SY MM TS. Performed the experiments: MA RS YA. Analyzed the data: MA RS TE SY MM TS. Contributed reagents/materials/analysis tools: MH KF YF. Wrote the paper: TS.

References

1. Granucci F, Zanoni I, Ricciardi-Castagnoli P (2008) Central role of dendritic cells in the regulation and deregulation of immune responses. Cell Mol Life Sci 65: 1683–1697.
2. Gerosa F, Baldani-Guerra B, Nisii C, Marchesini V, Carra G, et al. (2002) Reciprocal activating interaction between natural killer cells and dendritic cells. J Exp Med 195: 327–333.
3. Seya T, Matsumoto M (2009) The extrinsic RNA-sensing pathway for adjuvant immunotherapy of cancer. Cancer Immunol Immunother 58: 1175–1184.
4. Akazawa T, Okuno M, Okuda Y, Tsujimura K, Takahashi T, et al. (2007) Antitumor NK activation induced by the Toll-like receptor3-TICAM-1 (TRIF) pathway in myeloid dendritic cells. Proc Natl Acad Sci USA 104: 252–257.
5. Miyake T, Kumagai Y, Kato H, Guo Z, Matsushita K, et al. (2009) Poly I:C-induced activation of NK cells by CD8 alpha+ dendritic cells via the IPS-1 and TRIF-dependent pathways. J Immunol 183: 2522–2528.
6. McCartney S, Vermi W, Gilfillan S, Cella M, Murphy TL, et al. (2009) Distinct and complementary functions of MDA5 and TLR3 in poly(I:C)-mediated activation of mouse NK cells. J Exp Med;Dec. 14.
7. Haller D, Serrant P, Granato D, Schiffrin EJ, Blum S (2002) Activation of human NK cells by staphylococci and lactobacilli requires cell contact-dependent costimulation by autologous monocytes. Clin Diagn Lab Immunol 9: 649–657.
8. Chavakis T, Preissner KT, Herrmann M (2007) The anti-inflammatory activities of *Staphylococcus aureus*. Trends Immunol 28: 408–418.